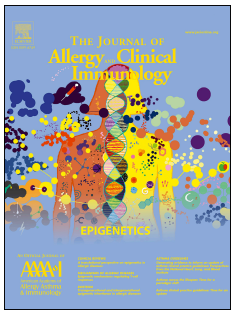
# Accepted Manuscript




Tolerogenic signalling of alveolar macrophages induces lung adaptation to oxidative injury

Benoit Allard, PhD, Alice Panariti, PhD, Erwan Pernet, PhD, Jeffrey Downey, MSc, Satoshi Ano, MD PhD, Marieme Dembele, MSc, Emily Nakada, PhD, Utako Fujii, MD PhD, Toby K. McGovern, PhD, William S. Powell, PhD, Maziar Divangahi, PhD, James G. Martin, MD DSc

PII: S0091-6749(19)30963-7

DOI: https://doi.org/10.1016/j.jaci.2019.07.015

Reference: YMAI 14100

To appear in: *Journal of Allergy and Clinical Immunology*

Received Date: 19 July 2018

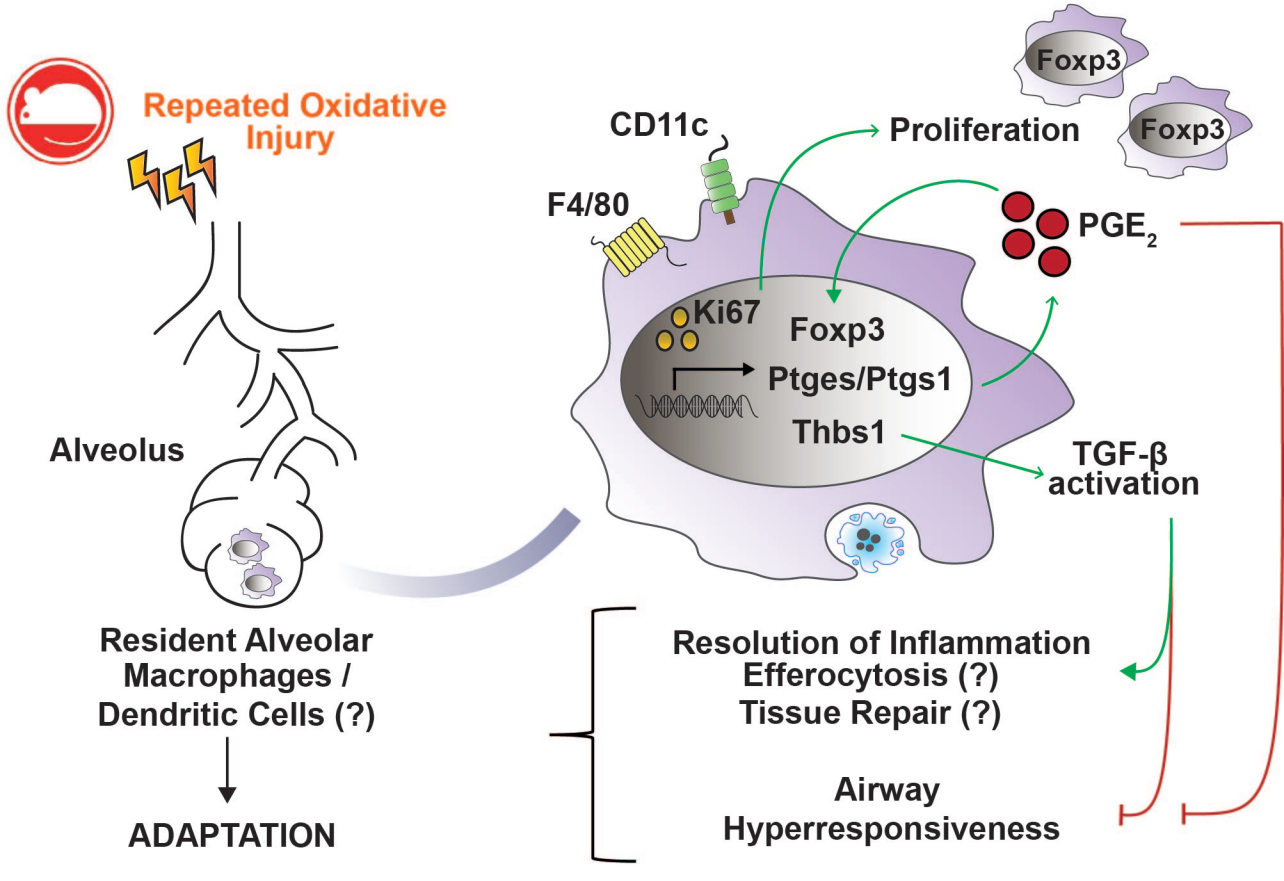
Revised Date: 6 July 2019

Accepted Date: 12 July 2019

Please cite this article as: Allard B, Panariti A, Pernet E, Downey J, Ano S, Dembele M, Nakada E, Fujii U, McGovern TK, Powell WS, Divangahi M, Martin JG, Tolerogenic signalling of alveolar macrophages induces lung adaptation to oxidative injury, *Journal of Allergy and Clinical Immunology* (2019), doi: https://doi.org/10.1016/j.jaci.2019.07.015.

This is a PDF file of an unedited manuscript that has been accepted for publication. As a service to our customers we are providing this early version of the manuscript. The manuscript will undergo copyediting, typesetting, and review of the resulting proof before it is published in its final form. Please note that during the production process errors may be discovered which could affect the content, and all legal disclaimers that apply to the journal pertain.

# Adaptation to repeated oxidative stress-induced lung injury mediated by resident alveolar macrophages signalling



ACCEPTED MANUSCRIPT

# Title: Tolerogenic signalling of alveolar macrophages induces lung adaptation to oxidative injury

**Authors:** Benoit Allard PhD, Alice Panariti PhD, Erwan Pernet PhD, Jeffrey Downey MSc, Satoshi Ano MD PhD, Marieme Dembele MSc, Emily Nakada PhD, Utako Fujii MD PhD, Toby K McGovern PhD, William S Powell PhD, Maziar Divangahi PhD and James G Martin* MD DSc

**Affiliations:**
Meakins Christie Laboratories, Research Institute of the McGill University Health Centre, and the Department of Medicine, McGill University, Montreal, Quebec, Canada

*Corresponding Author:

James G. Martin, M.D., D.Sc.
Meakins-Christie Laboratories
Research Institute of the McGill University Health Centre
Block E, Room EM3.2379
1001 Décarie Blvd
Montreal, QC, H4A 3J1
Tel: (514) 934-1934 ext 76298
Fax: (514) 933-3962
Email: james.martin@mcgill.ca

**Author contributions:** B.A. designed the research; performed experiments; collected, analyzed, and interpreted data; and wrote the manuscript. A.P., E.P., J. D., S.A., M.D., E.N., U.F., T.K.M. performed experiments and analyzed data and W.S.P., supervised experiments and analyzed data. M.D. and J.G.M. supervised the work, analyzed data, and revised the final manuscript.

**Competing interests**: The authors declare that they have no competing interests.

**Funding:** This study was funded by an operating grant from the Canadian Institutes of Health Research (MOP-126131) and the Richard and Edith Strauss Foundation.

**Key words:** Lung injury; oxidative stress; disease tolerance; lung function adaptation; Foxp3; alveolar macrophages; mucosal immunology.

ACCEPTED MANUSCRIPT

**Key messages:**

- Residential alveolar macrophages, but not bone marrow-derived monocytes, mediate adaptation to oxidative stress-induced lung injury.
- A subset of highly proliferative alveolar macrophages expressing Foxp3 has tolerogenic signatures that are linked to preservation of lung function following oxidative injury.
- $Foxp3^+$ alveolar macrophages may mediate their effects in part through $PGE_2$, for adaptation of airway dysfunction affecting the large conducting airways.
- $Foxp3^+$ alveolar macrophages increase expression of thrombospondin, the main activator of TGF-β, and neutralization of TGF-β enhances both inflammation and airway hyperresponsiveness.

**Abbreviations used:**

AHR: airway hyperresponsiveness
BAL: bronchoalveolar lavage
CCR2: C-C chemokine receptor type 2
$Cl_2$: chlorine
DTR: diphtheria toxin receptor
FDR: false discovery rate
Foxp3: forkhead box P3
GSH: reduced glutathione
GSSG: oxidized glutathione
Nrf2: nuclear factor, erythroid derived 2, like 2
$PGE_2$: prostaglandin $E_2$
Ptgs1: Prostaglandin-Endoperoxide Synthase 1 (COX1)
Rag-1: recombination activating gene 1
RFP: red fluorescent protein
TAC: total antioxidant capacity
TGF-β: transforming growth factor-beta
Thbs1: thrombospondin 1
Tregs: regulatory T cells

ACCEPTED MANUSCRIPT


## ABSTRACT

**BACKGROUND:** Inhaled oxidative toxicants, present in ambient air, cause airway epithelial injury, inflammation and airway hyperresponsiveness. Effective adaptation to such environmental insults is essential for the preservation of pulmonary function whereas failure or incomplete adaptation to oxidative injury may render the host susceptible to the development of airway disease.

**OBJECTIVE:** To explore the mechanisms of airway adaptation to oxidative injury.

**METHODS:** For the model to the study of pulmonary adaptation to oxidative stress induced-lung injury we exposed mice to repeated nose-only chlorine gas exposures. Outcome measures were evaluated 24h after the last chlorine exposure. Lung mechanics and airway responsiveness to methacholine were assessed using FlexiVent®. Inflammation and anti-oxidant responses were assessed in both bronchoalveolar lavage and lung tissue. Using loss-of-function or gain-of-function as well as genomic approaches, we further dissected the cellular and molecular mechanisms involved in pulmonary adaptation.

**RESULTS:** Repeated exposures to oxidative stress resulted in pulmonary adaptation evidenced by abrogation of neutrophilic inflammation and airway hyperresponsiveness. This adaptation was independent of antioxidant mechanisms and regulatory T cells, but dependent on residential alveolar macrophages. Interestingly, 5% of alveolar macrophages expressed Foxp3 and depletion of these cells abolished adaptation. Results from transcriptomic profiling and loss-and-gain of function suggest that adaptation may be dependent on transforming growth factor-β (TGF-β) and prostaglandin $E_2$ ($PGE_2$).

**CONCLUSION:** Pulmonary adaptation during oxidative stress-induced lung injury is mediated by a novel subset of $Foxp3^+$ alveolar macrophages that limits inflammation favoring airway adaptation and host fitness via TGF-β and $PGE_2$.

ACCEPTED MANUSCRIPT

**Capsule Summary:**

Alveolar macrophages drive protection to repeated oxidative injury through modification of their phenotype, including Foxp3 expression. Inability to develop this subpopulation may promote susceptibility to airway disease.

ACCEPTED MANUSCRIPT

ACCEPTED MANUSCRIPT

## INTRODUCTION

Industrialization and Westernization have radically changed the quality of ambient air, introducing a range of particulate and non-particulate pollutants that are reflected in the burden of respiratory disease (1, 2). Ozone, oxides of nitrogen and sulphur dioxide are well known pollutants but another important environmental irritant is chlorine ($Cl_2$), encountered in swimming pools and resulting from inappropriate mixing of domestic cleaning products. Massive exposures to $Cl_2$ have resulted from spillages during transport (3) and use in recent terrorist attacks (4). A common feature of the inhalation of pollutants is the induction of oxidative stress and oxidative airway injury, causing *de novo* airways disease or worsening the symptoms of pre-existing respiratory disease (5, 6). The public health significance of impaired airway function, whatever the cause, is substantial since it is a strong determinant of risk of a variety of diseases, including cardiovascular disease (7).

Oxidative injury triggers a predominantly neutrophilic inflammation (8) that further adds to the burden of the oxidative stress-mediated airway injury through the production of hypochlorite and other reactive species. Indeed, although neutrophils are important in combating infection, their presence in “sterile inflammation” or in exuberant inflammation is recognized to be deleterious for tissue integrity (9). Depletion of neutrophils prior to $Cl_2$ exposure abrogates airway dysfunction in mice (10), confirming the important pathological influence of the neutrophilic infiltration of the airways. Thus, mechanisms limiting damage and restoring tissue homeostasis are crucial in preventing the development of respiratory disease. Often the

113 airways are not subject to a single injurious exposure but may rather to repeated injury.
114 Repeated ozone exposures evoke an effective adaptation of the lungs, preserving lung function
115 (11). Mechanisms driving such adaptation have not been well explored and may be distinct
116 from those resolving inflammation (12). Although exposure to air pollution is common to all,
117 only a fraction of the population develops respiratory disease, suggesting the hypothesis that
118 failure to adapt may be a possible basis for disease susceptibility.
119
120 Several cell types have been implicated in inhibiting or terminating inflammation. Among these
121 cells, regulatory T cells (Tregs) have been extensively studied in relation to their role in reducing
122 inflammation in a variety of inflammatory diseases (13). In the context of airway disease, Tregs
123 have been reported to resolve inflammation and prevent airway hyperresponsiveness (AHR) in
124 an allergen model of asthma by an IL-10-dependent pathway (14). Following
125 lipopolysaccharide-induced acute lung injury in the mouse, Tregs are responsible for the
126 resolution of inflammation through a transforming growth factor (TGF)-β dependent pathway
127 (15). However, macrophages are also effectors of the resolution of inflammation (16, 17)
128 through effective phagocytosis of apoptotic cells, preventing dying cells from releasing pro-
129 inflammatory and toxic contents while triggering the release of anti-inflammatory and repair
130 factors (18). The adaptive mechanisms of macrophages have been reviewed extensively (19).
131 However, it is still unknown how lung macrophages regulate host tolerance to injurious
132 exposures.
133

In the current study, we have investigated the process of adaptation to oxidative stress-induced airway injury in the murine model of irritant asthma triggered by inhaled $Cl_2$. Hydration of $Cl_2$ in airway lining fluid forms hypochlorous acid, a highly reactive product, which is also released from activated neutrophils by the action of myeloperoxidase (20). Such oxidative stress leads to epithelial damage, exaggerated bronchoconstriction to inhaled methacholine, and a brisk neutrophilic inflammation (10). However, recovery from a single inhalational exposure to $Cl_2$ is largely complete by three days in the mouse (21), indicating an effective clearance of inflammatory cells and the restoration of the airway epithelium. Now we have examined if repeated exposures to $Cl_2$ lead to adaptation and, if so, by what mechanisms. Our study demonstrated a rapid adaptation of mice after three $Cl_2$ exposures, characterized by normalization of airway function, rapid epithelial repair, a marked reduction in inflammation and resistance to the effects of subsequent exposure to $Cl_2$. Such adaptation was mediated neither by the antioxidant response nor by Tregs, but rather by a subpopulation of alveolar macrophages that express Foxp3. Our findings suggest a role for $PGE_2$ and a potential role for TGF-β in adaptation to $Cl_2$.

ACCEPTED MANUSCRIPT

## MATERIALS AND METHODS

### Mice

BALB/c and C57BL/6 mice (8–12-week-old) were purchased from Charles River (Saint Constant, QC, Canada) or Jackson Lab (Sacramento, CA, USA). Mice were housed in a conventional animal facility at McGill University. All mice were treated in accordance with the guidelines of the Canadian Council for Animal Care, and protocols were approved by the Animal Care Committee of McGill University. *Nrf2*$^{-/-}$ mice were generated as described previously (22) and provided by the University of Tsukuba, Japan. CD11c DTR mice (B6.FVBTg(Itgax-DTR/EGFP)57Lan/J), DEREG mice (C57BL/6-Tg(Foxp3-DTR/EGFP)23.2Spar/Mmjax), FOXP3-IRES-mRFP mice (C57BL/6-Foxp3$^{tm1Flv}$/J), *Rag1*$^{-/-}$ mice (B6.129S7-Rag1$^{tm1Mom}$/J), *Ccr2*$^{-/-}$ mice (B6.129S4-*Ccr2*$^{tm1Ifc}$/J) and *Ptges*$^{-/-}$ mice (B6.129S6-*Ptges2*$^{tm1Bhk}$/J) were purchased from Jackson Laboratories and bred in-house.

### Chlorine exposure

Chlorine ($Cl_2$) gas was mixed with room air using a standardized calibrator (Dynacalibrator, Model23023A, VICI Metronics, Poulsbo, WA, USA) at a concentration of 100 ppm for BALB/c or 400 ppm for C57BL/6. Mice were subjected to nose-only exposure to $Cl_2$ gas (duration 5 minutes for BALB/c and 4 minutes for C57BL/6) once or 3 times at an interval of 84 hours. Mice were studied 24 hours following the last $Cl_2$ exposure.

**Measurements of airway responsiveness**

Measurement of respiratory system mechanics was performed as previously described (23). Briefly, anesthetized mice were connected to a mechanical ventilator (FlexiVent, Scireq, Montreal, QC, Canada), and aerosolized methacholine (Sigma-Aldrich, St. Louis, MO, USA) was administered at increasing concentrations (6.25–50 mg/ml).

**Bronchoalveolar lavage**

Bronchoalveolar lavage (BAL) was performed with a single instillation of 1 ml of cold phosphate buffered saline with bovine serum albumin (PBS/BSA1%) via the tracheal cannula after the measurements of respiratory mechanics. The total number of cells was counted in a Neubauer chamber, and the differential cell count was determined after staining of cytospin slides with HEMA 3 STAT PACK (Fisher Scientific, Saint-Laurent, QC, Canada). The cell differential was determined from a count of 300 cells. The BAL supernatant was stored at -80°C for further analysis.

**Immunohistochemistry**

Mice were euthanized with an overdose of pentobarbital (CEVA Santé Animale, Libourne, France). The pulmonary circulation was flushed with sterile saline via the right ventricle until the effluent was clear. Lungs were inflated and fixed with 10% formalin, and embedded in paraffin. Adjacent tissue sections (4µm) were de-paraffinized in xylene, rehydrated through a decreasing ethanol gradient, and rinsed in PBS before staining with hematoxylin and eosin or

being processed for detection of proliferation or apoptosis as described below. For the staining of proliferative nuclei, tissue sections were processed for antigen unmasking in 10 mM citrate buffer pH 6 and permeabilization in 0.2% Triton X-100 (Sigma-Aldrich). Endogenous peroxidase activity was blocked with 6% hydrogen peroxide for 30 min at room temperature and subsequently blocked in universal blocking solution (DakoCytomation, Glastrop, Denmark). Monoclonal antibody for proliferating cell nuclear antigen (PCNA, CalBiochem) was applied overnight at 4°C and then detected with biotinylated horse anti-mouse IgG, avidin/biotin-alkaline phosphatase complex and Vector Red chromogen substrate (Vector Laboratories, Burlington, ON, Canada). For the negative control, primary antibody was replaced by mouse IgG2a. Apoptosis was detected by TUNEL with an ApopTag peroxidase kit (EMD Millipore) and enhanced DAB (Dako) following manufaturer's instructions. Nuclei were counterstained with 0.5% (w/v) methyl green. Microscope slides were scanned at x20 (Ariol scanner, Leica Biosystems, San Diego, CA, USA) and blindly analyzed with Aperio ImageScope 12.3 software (Leica Biosystems). For each section, 15-20 airways were considered for the analysis. The airways were analyzed when at least 50% of the epithelium where intact. Very large conducting airways were excluded from the analysis. The number of epithelial nuclei positive for PCNA or TUNEL were counted and expressed per mm of the length of the epithelium.

**Measurement of glutathione**

Reduced glutathione (GSH) and the oxidized form (GSSG) were measured in BAL and lung homogenized supernatants. The superior lobes of the right lung were homogenized in 0.2 M

212 phosphoric acid. Homogenates were then centrifuged at 10,000 × g for 5min at 4◦C. As
213 previously described (24, 25), GSH and GSSG were measured by RP-HPLC using a post-column
214 derivatization procedure modified from the literature (26).
215
216 **Total anti-oxidant capacity**
217 Total antioxidant capacity (TAC) was measured in both BAL fluid supernatant and lung
218 homogenized supernatants. TAC was assessed using a colorimetric assay according to the
219 manufacturer's instructions (Bio-Vision, Milpitas, CA, USA).
220
221 **RNA isolation and Q-RT-PCR**
222 Twenty-four hours following the last $Cl_2$ exposure, the right lung lobe was placed in a 1.5ml
223 tube, snap-frozen in liquid nitrogen, and stored at -80°C. Subsequently, RNA was extracted
224 using the RNeasy Mini Kit (Qiagen, Mississauga, ON, Canada). Following RNA isolation, cDNA
225 was synthesized with AffinityScript QPCR cDNA Synthesis Kit (Agilent Technologies, Santa Clara,
226 CA, USA). A total of 100ng of total RNA was reverse-transcribed into cDNA. For quantitative
227 real-time PCR, iTaq Universal SYBR Green Supermix (Bio Rad, Hercules, CA, USA) was used with
228 the Applied Biosystems 7500 Fast Real-Time PCR system. Transcripts for the following genes
229 were evaluated; *cat* (L: ccttcaagttggttaatgcaga; R: caagtttttgatgccctggt), *sod3* (L:
230 ctcttgggagagcctgaca; R: gccagtagcaagccgtagaa), *gpx3* (L: acaattgtcccagtgtgtgc; R:
231 accatccctgggtttcaag), *txnrd1* (L: ttttgtcacaccgactcctct; R: ccacattcacacacgttcct), *Foxp3* (L:
232 actcgcatgttcgcctactt; R: gtccacactgctcccttctc), *Ptgs1* (L: aggcactggtggatgccttc; R: aagggctgtaggcgcatct),

233 *Ptges* (L: ggatgcgctgaaacgtgga ; R: caggaatgagtacacgaagcc), *Thbs1* (L: cacctctccgggttactgag; R:
234 gcaacaggaacaggacaccta) and *s9* (L: atccgccaacgtcacatta; R: tcttcactcggcctggac) was used as a
235 reference gene. For all PCRs, normalization was done by using a calibrator sample to allow for
236 comparison between multiple PCRs.
237
238 **Lung Digest**
239 Following pentobarbital-induced euthanasia, lungs were removed from the chest and cut into
240 small pieces in 2ml of RPMI (Life technologies, Carlsbad, CA, USA) in one well of a six well plate
241 (Sarstedt, Nümbrecht, Germany). 2mL of collagenase (SigmaAldrich) at 300U/mL (final
242 concentration 150U/mL) was added to the well and incubated at 37˚C for 1h. A 10ml syringe
243 (BD, Franklin Lakes, New Jersey, USA) with a 16G1 needle (BD) was used to disperse the tissue
244 further. The suspension was passed through a 40µm nylon cell strainer (VWR, Radnor,
245 Pennsylvania, USA) on a 50mL tube (Sarstedt). Cells were centrifuged for 10 minutes at
246 1500rpm and the supernatant was discarded. Red blood cell lysis was performed by adding 2mL
247 of RBC lysis buffer (Biolegend, San Diego, CA, USA). After 2 minutes of incubation, the reaction
248 was stopped by adding RPMI up to 25mL. The tube was centrifuged 10 minutes at 1500rpm and
249 the supernatant was discarded. Cells were counted with a Neubauer chamber and $3.10^6$ cells
250 were placed per tube.

**Flow cytometry**

Flow cytometry was performed on BALs obtained by instilling 1 ml of PBS intra-tracheally, or on single cells from digested lungs. Cells were resuspended in 100µl of PBS with e780 (dilution 1/1000) (Fixable Viability Dye eFluor® 780, eBioscience, San Diego, CA, USA) for viability dye staining, and incubated for 15 minutes at room temperature in the dark. Samples were washed with 1ml of FACS buffer (PBS/BSA 1%) and centrifuged at 1500 rpm, 5 minutes, 4˚C. Cells were re-suspended in 25µl of FACS buffer with Fc Block (anti-mouse CD16/32, TruStain fcX, Biolegend) and incubated for 10 minutes in the dark on ice. A mix of antibodies was added directly per tube (25µl/tube for a final volume of 50µl/tube) and incubated for 30 minutes in the dark on ice. Inflammatory cells were surface-stained with different combinations of antibodies (anti-mouse CD4-PerCP, clone RM4-5, BioLegend, San Diego, CA, USA; and anti-mouse CD25-PE, clone PC 61, BD Biosciences, San Jose, CA, USA; or different combinations of anti-mouse CD11c-PerCP, clone N418; and anti-mouse F4/80-PE/Cy7, clone BM8, from BioLegend; anti-mouse CD11c-APC, clone HL3; anti-mouse Siglec-F-PE, clone E50-2440; anti-mouse Ly6G-FITC, clone 1A8; anti-mouse CD3-BV786, clone 145-2C11; and anti-mouse B220-PerCP-Cy5.5, clone RA3-6B2; anti-mouse NK1.1-BV650, clone PK136, from BD Biosciences). Samples were washed with 1ml of FACS buffer. Cells were fixed, permeabilized and stained for Foxp3 using the Foxp3/Transcription Factor Staining Buffer Set (#00-5523-00, eBioscience) beginning with the re-suspension of cells in 250µl of Fixation/Permeabilization buffer and incubating for 30 minutes in the dark on ice. Samples were washed with 1ml of the

permeabilization buffer with BSA 1%. Cells were re-suspended in 50µl of permeabilization buffer with BSA 1% and intracellularly stained (anti-mouse/rat Foxp3-APC, clone FJK-16s; or anti-Ki67-eFluor660, clone SolA15, from eBioscience) and incubated for 30 minutes in the dark on ice. Samples were washed with 1ml of permeabilization buffer. Samples were transferred to FACS tubes with a cell strainer cap (#352235, Corning, NY, USA). Cells were re-suspended in 350µl of PBS and $1.10^6$ cells were acquired with the BD FACSCanto II (BD Biosciences). Compensation was performed with beads (UltraComp eBeads, eBiosciences) and a fluorescence minus one strategy was used as controls(27) or an isotype control antibody when appropriate. Analysis was performed with FlowJo software 10.1r5 (Ashland, OR, USA).

**Macrophage Isolation by lung digestion and adherence**

Foxp3 expression was assessed in an enriched macrophage population from digested lungs. A single cell suspension of pooled lungs from $Cl_2$x3-exposed, FOXP3-IRES-mRFP mice (C57BL/6-Foxp3$^{tm1Flv}$/J) was prepared using the lung digest protocol detailed in the lung digest section, with the following modifications: DNase I (11284932001, Sigma-Aldrich) was added to the collagenase lung digest cocktail at a final concentration of 10µg/ml and red blood cells were lysed with ACK lysis buffer (A1049201, Fisher Scientific) for 5 minutes on ice. Following lung digestion, macrophages were enriched by plating lung cells on tissue culture plates (#667651, Ultident) for 1 hour to allow macrophages to adhere, followed by 2 washes with PBS to remove non-adherent cells. Enriched macrophages were collected following a 15-minute incubation at 37°C with Accutase™ (SCR005, Fisher Scientific). Accutase™ was inactivated with an equal

volume of RPMI medium containing FBS, centrifuged, re-suspended in FACS buffer, and divided into tubes to be stained and assessed by flow cytometry. Enriched macrophages were first stained with Fixable Viability Dye eFluor® 780 (eBioscience); followed by anti-mouse F4/80-APC, clone BM8 and anti-mouse CD11c-BV421, clone N418 (BioLegend). Samples were stained intracellularly with anti-mouse Foxp3-PE-Cy7, clone 3G3 (Abcam, Cambridge, UK) using the flow cytometry staining protocols detailed in the Flow Cytometry section to assess double positive Foxp3 expression (endogenous Foxp3-RFP and Foxp3-PE-Cy7) within the $RFP^+$ alveolar macrophage ($F4/80^+CD11c^+$) population using the BD FACSCanto II. Compensation, control strategies, and the analysis program were previously described (Flow Cytometry Section).

**Cell depletion**

For Foxp3 positive cell depletion in DEREG mice, diphtheria toxin (#150, List Biological Laboratories, Campbell, CA, USA) was administered by i.p. 12 hours before each $Cl_2$ exposure at a concentration of 40ng/g body weight. For CD11c positive cell depletion in CD11c DTR mice, diphtheria toxin (List Biological Laboratories) was administered i.p. 12 hours before the last $Cl_2$ exposure at a concentration of 20ng/g. Macrophage depletion was also performed by administration of clodronate liposome (Encapsula NanoSciences, Nashville, USA) 24 hours before the last $Cl_2$ exposure, at concentrations of 250µg/50µl i.n. plus 250µg/100µl i.v.. Liposome alone was used as control.

**TGF-β neutralization**

Neutralizing monoclonal TGF-β 1/2/3 antibody (1D11) (MAB1835-500, Novus, St Charles, Missouri, USA) or IgG1 isotype control (11711) (MAB002, Novus) were injected i.p. just before the last $Cl_2$ exposure at a concentration of 5mg/kg body weight in sterile PBS at concentration of 250ng/µl.

**Adoptive transfer of macrophages**

Unexposed (naïve) and repeatedly exposed (adapted) mice were euthanized by an overdose of pentobarbital. A metal cannula was placed in the trachea in order to perform BAL. The abdominal aorta was sectioned to reduce the blood in the lungs. The heart and lungs were gently removed *en bloc* from the chest, still connected to the cannula. One ml of cold PBS/EDTA 1mM was injected into the lung. The injection of PBS was repeated until the collection reached 10ml. To increase the number of alveolar macrophages collected, the lung was gently massaged before aspirating the lavage fluid. Tubes were centrifuged at 1500rpm, 5min, 4°C. The pellets were pooled per groups of mice (naïve vs adapted). Cell count was done with a Neubauer chamber. Cells were stained for viable alveolar macrophages ($e780^-$, $F4/80^+$, $CD11c^+$) to be sorted with a BD FACSAria Fusion (BD). After the cell sorting, macrophages were washed twice with sterile PBS and re-suspended at 250 000 cell/50µl for transfer into naïve mice. To cell sort viable $Foxp3^+$ and $Foxp3^-$ alveolar macrophages, we used Foxp3-RFP mice (Foxp3 is co-expressed with a monomeric red fluorescent protein). Sorted alveolar macrophages were transferred by intra-tracheal instillation (BD Angiocath, ref 381123) to naïve mice under isoflurane anesthesia. The skin was carefully closed with a sterile staple. Mice were returned to

335 their cages and recovered quickly. Twenty-four hours after the adoptive transfer, mice were
336 challenged with a single $Cl_2$ exposure.
337
338 **Gene array analysis**
339 Sorted alveolar macrophages from adapted and naïve mice were also used for transcriptomic
340 analysis. 1 ml of TRIzol® Reagent (Life Technologies) was added on the pellet (about 1 000 000
341 of cells/tube to compare naïve and adapted alveolar macrophages). Cells were lysed by
342 repeated pipetting. Homogenized samples were stored at -80°C. When the number of required
343 samples was reached, all samples were thawed for subsequent procedure. After 5 minutes at
344 room temperature, 0.1 ml of 1-bromo-3-chloropropane (BCP – Phase Separation Reagent, MRC,
345 Cincinnati, OH, USA) was added per tubes. Tubes were shaken vigorously and incubated at
346 room temperature for 2 minutes. Samples were centrifuged at 12 000g for 15 minutes at 4°C.
347 The aqueous phase was removed and 400µl was then used on the RNeasy Mini Kit (Qiagen) to
348 complete the RNA extraction. RNA samples were processed by Genome Quebec (McGill
349 University) with an Affymetrix Mouse Gene 2.0 ST (Affymetrix, Santa Clara, CA, USA). Analysis of
350 the gene array was performed with Expression Control™ software (Affymetrix) and the
351 Transcriptome Analysis Consol™ software (Affymetrix).
352
353 **Statistical analysis**
354 We used GraphPad Prism version 5.0 (San Diego, CA, USA) to generate figures and statistical
355 analyses. Data are shown as mean ± 1 standard error of the mean. Data were analyzed using

356 one-way ANOVA and the post hoc analysis with Newman-Keuls test. Experiments evaluating
357 respiratory system mechanics were analyzed using two-way ANOVA, and post hoc analysis was
358 performed with a Bonferroni multiple-comparison test. Mann Whitney U test was used when
359 appropriate. A P value $< 0.05$ was considered significant.
360

ACCEPTED MANUSCRIPT

ACCEPTED MANUSCRIPT

## RESULTS

### Repeated oxidative injury leads to rapid protective airway adaptation

We previously demonstrated that a single exposure of mice to the potent airway irritant $Cl_2$ resulted in AHR to inhaled methacholine accompanied by a predominantly neutrophilic airway inflammation and the effects were abrogated by anti-oxidant treatments (28) and neutrophil depletion (10). To determine whether murine airways are able to adapt to repeated oxidative injury, we examined the effect of multiple nose-only exposures to $Cl_2$ gas (Fig 1A). Interestingly, three exposures of $Cl_2$ induced a dramatic attenuation of the AHR that was present after a single exposure (Fig 1B), as well as a reduction of the overall burden of inflammatory cells in the airways (Fig 1E). There was no difference in number of macrophages (Fig 1C), there was a significant attenuation of neutrophilia (Fig 1D) in the group of mice that received three exposures to $Cl_2$ compared to a single exposure. We further corroborated these findings by flow cytometry (Fig 1F) and similarly observed, while there was no significant difference in macrophages (Fig 1G), there was a significant reduction in neutrophils (Fig 1H). Eosinophils and lymphocytes were also present in the BAL but were much fewer in number than macrophages and neutrophils (Fig E1B). Further investigation of the mechanical properties of the airway tree using a model that permits attribution of changes in different parts of the respiratory tract (29) demonstrated that the improvement in AHR was attributable to the effects on both large and small airways as well as the dynamic lung tissue stiffness (Fig E1A). We explored the duration of protection in mice exposed to $Cl_2$ a month following the initial three exposures. These mice also

showed attenuated responses to $Cl_2$, showing only a minor increase in response to methacholine challenge and in airway neutrophilia (Fig E2).

We investigate next the impact of $Cl_2$ on the integrity of airway epithelial cells. In three times-exposed mice, the number of apoptotic epithelial cells (TUNEL staining) was lower than in mice that underwent a single exposure (Fig 2A and C) and there was a concurrent enhancement of the proliferation (PCNA staining) of epithelial cells (Fig 2B and D). We next extended our results to another mouse strain (BALB/c) that is more susceptible to $Cl_2$ challenge (100ppm evokes a comparable response to 400ppm for C57BL/6) (21, 25). Similar adaptation to $Cl_2$ was also observed with BALB/c mice (Fig E1C-E). Collectively, these results show that upon multiple injurious exposures to the airway irritant $Cl_2$, the airways manifest a rapid and effective adaptation that restores lung function, attenuates airway neutrophilia and promotes epithelial cell hyperplasia, that extends to two strains differing in genetic background and susceptibility to $Cl_2$. Thus, from here on we will refer to mice 3 times exposed to $Cl_2$ as "adapted" mice.

**Airway adaptation is independent of the anti-oxidant response**

Based on the therapeutic effects of an anti-oxidant administered or an hour after inhalation of $Cl_2$ (23, 28) we reasoned that an enhanced anti-oxidant response might account for adaptation to repeated oxidative insult. We first quantified reduced (GSH) and oxidized glutathione (GSSG) in the bronchoalveolar lavage. Both GSH (Fig 3A) and GSSG (Fig 3B) levels were equal to steady-state levels in the BAL and the GSH:GSSG ratio was also not significantly altered (Fig 3C). Results

402 were similar for the lung parenchyma, and again no statistically significant differences were
403 found (Fig E3A). Moreover, detoxifying enzymes were not increased in association with
404 adaptation, but instead, the *nuclear factor, erythroid derived 2, like 2* (*Nrf2)*-dependent
405 enzymes superoxide dismutase-3 and glutathione peroxidase-3 were significantly lower in
406 expression in adapted mice compared to a single exposure (Fig E3B). Although there was no
407 significant difference in the total anti-oxidant capacity of BAL fluid between adapted and
408 unexposed mice (Fig E3C), we further explored if other aspects of the anti-oxidant response
409 were important in adaptation. Thus, we assessed the responses of mice deficient in ~~2~~*Nrf2*$^{-/-}$ that
410 are known to have a broadly defective anti-oxidant response (22). However, the airway
411 adaptation was intact in *Nrf2*$^{-/-}$ mice compared to controls with the same (BALB/c) genetic
412 background (Fig 3D-F). Taken together, these findings indicate that the anti-oxidant response
413 was not responsible for the $Cl_2$ induced airway adaptation.
414
415 **Airway adaptation is dependent on Foxp3, but not on regulatory T cells**

416 Considering that AHR following $Cl_2$ exposure is predominantly driven by airway neutrophilia
417 (10), which is substantially suppressed in adapted mice, we sought to address the potential
418 cellular mechanisms involved in its suppression. Several studies have previously demonstrated
419 that $CD4^+$ $CD25^+$ $Foxp3^+$ regulatory T cells (Tregs) can reduce neutrophilia (30-32). Moreover,
420 Tregs have been shown to be equally important in the resolution phase of lipopolysaccharide-
421 induced acute lung injury (15), as well as infectious diseases (33, 34). To assess the possible role
422 of Foxp3-expressing cells in airway adaptation, we first used DEREG mice (35, 36) and

confirmed virtually complete depletion of Tregs by the administration of diphtheria toxin to these mice (Fig 4A and gating strategy Fig E4A). Diphtheria toxin did not alter the composition of the BAL cells in both air-exposed and single-exposed mice (Fig 4C, D and E4B). Depletion of $Foxp3^+$ cells abrogated the airway adaptation and restored AHR, and neutrophilic inflammation following three exposures to $Cl_2$ (Fig 4B-D).

As the frequency of Tregs was diminished after a single exposure to $Cl_2$ and restored after three exposures (Fig 4A, right most panel), and Tregs are the principal cells that express Foxp3, we anticipated that Tregs were responsible for this adaptation. To address this possibility, we performed similar experiments in *Rag1*$^{-/-}$ mice that lack all mature T and B cells, including Tregs (37). Despite the lack of Tregs, the *Rag1*$^{-/-}$ mice adapted at both the functional (AHR) and cellular (neutrophilia) levels (Fig 4E-G).

**Airway adaptation is dependent on resident alveolar macrophages**

We next investigated the potential contribution of innate immunity to adaptation. Pulmonary macrophages have been shown to play important role in the regulation of airway inflammation (17) and to prevent AHR (38). We next examined the potential contribution of pulmonary macrophages to the regulation of adaptation to $Cl_2$ exposure. Alveolar macrophages ($SiglecF^+$ $CD11c^+$ $CD11b^-$) have a self-renewal capacity but during inflammation, bone marrow derived inflammatory monocytes ($CD11b^+Ly6C^+$ $CD11c^-$) are recruited into the lung in a Ccr2-dependent manner. To investigate the role of alveolar macrophages versus recruited macrophages in the

443 adaptation to $Cl_2$, we first depleted $CD11c^+$ cells that include alveolar macrophages, but not
444 recruited macrophages (39), from CD11c DTR mice with diphtheria toxin. Treatment with
445 diphtheria toxin resulted in approximately 70% depletion of alveolar macrophages (Fig E5B-C)
446 whereas $CD11b^+F4/80^+$ monocytes/macrophages were not affected (Fig E5D). Importantly this
447 alveolar macrophage depletion abrogated adaptation, as it was accompanied by a significantly
448 increased AHR (Fig 5A) and airway neutrophilia (Fig 5C) in repeated $Cl_2$-exposed mice. The
449 administration of diphtheria (40ng/g i.p.) to air-exposed mice did not alter the cell differential
450 of BAL fluid nor cause an increase in the inflammatory response after 1 exposure to $Cl_2$ (Fig
451 E5A). We assessed also the effects of diphtheria toxin on the inflammatory cells in the lung
452 tissues. There was a reduction in dendritic cells from 5.8 +/- 1.4 to 3.0 +/- 0.4, although the
453 reduction did not reach statistical significance (Figure E5D). NK/T/B lymphocytes, eosinophils
454 and neutrophils were not affected by the treatment (data not shown).
455
456 To interrogate further the role of alveolar macrophages, we depleted the airways of phagocytic
457 cells, including alveolar macrophages, using liposomal clodronate (Clodrosome®) delivered
458 systemically (i.v.) and locally (i.n.). Treatment with clodronate led to a reduction in alveolar
459 macrophages similar to that in the CD11c DTR experiments (Fig E5C), while the total numbers of
460 airspace macrophages were not significantly changed following $Cl_2$ exposure as clodronate had
461 no impact on the recruited macrophages (Fig 5E). Similar to depletion by diphtheria toxin in
462 CD11c DTR mice, clodronate depletion also resulted in restoration of $Cl_2$-induced AHR (Fig 5D)

463 and neutrophilia (Fig 5F). These results suggest that bone-marrow derived
464 monocyte/macrophages are not required for adaptation to repeated $Cl_2$ exposures.
465
466 To further explore a possible role for bone marrow-derived monocytes/macrophages in airway
467 adaptation, we exposed Ccr2-deficient mice (40) to $Cl_2$ and showed that the airway adaptation
468 was intact (Fig 5G). Additionally, total inflammatory cell counts were reduced in the adapted
469 mice compared to the one time-treated mice (Fig 5H), as anticipated, and this was
470 predominately attributable to neutrophil reduction (Fig 5J), but not macrophages (Fig 5I).
471 Importantly, while the total numbers of recruited macrophages ($CD11b^+$) were significantly
472 decreased in adapted Ccr2-deficient mice (Fig 5K, 5N and 5O), the frequency and total number
473 of alveolar macrophage populations was not significantly changed (Fig 5L-M). Thus, collectively,
474 these results indicate that airway adaptation is attributable to residential alveolar
475 macrophages.
476

477 **Airway adaptation is dependent on alveolar macrophages expressing Foxp3**

478 Since the depletion of $Foxp3^+$ cells in DEREG mice completely prevented adaptation
479 independently of Tregs and the depletion of alveolar macrophages also entirely abrogated
480 adaptation, we next investigated whether a subset of alveolar macrophages responsible for
481 adaptation expressed Foxp3. Although controversial, it has been suggested that macrophages
482 have the capacity to express Foxp3 (41). Approximately 5% of alveolar macrophages expressed
483 Foxp3, but only when harvested from $Cl_2$-adapted mice (Fig 6A and B). Additionally, the



ACCEPTED MANUSCRIPT

484 macrophages expressing Foxp3 were significantly decreased after diphtheria toxin treatment of
485 DEREG mice (Fig 6B) while the total alveolar macrophage population was not significantly
486 affected (Fig E6C). The level of Foxp3 expression in alveolar macrophages of adapted mice was
487 not significantly different at 24, 48 and 72 hours after the third $Cl_2$ exposure (Fig E6D). Foxp3
488 expression in alveolar macrophages was further confirmed by isolating alveolar macrophages
489 from the lungs of Foxp3-RFP mice. Cells were enriched from lungs that were digested into single
490 cells and cultured for one hour on tissue culture plates. Adherent cells were collected and
491 stained for F4/80 and CD11c. Cells were also stained intracellularly with a Foxp3-PE-Cy7
492 antibody. 13.9% of F4/80$^{+}$CD11c$^{+}$RFP$^{pos}$ cells also positively stained with the Foxp3-PE-Cy7
493 antibody compared to 1.66% of F4/80$^{+}$CD11c$^{+}$RFP$^{neg}$ cells (Fig 6C). We also noted a two-fold
494 increase in the mean fluorescence intensity of Foxp3-PE-Cy7 in all F4/80$^{+}$CD11c$^{+}$RFP$^{pos}$
495 (MFI=340) versus all F4/80$^{+}$CD11c$^{+}$RFP$^{neg}$ (MFI=174) populations.
496
497 To investigate the mechanism by which the F4/80$^{+}$CD11c$^{+}$Foxp3$^{+}$ cells accumulated in the
498 airways of adapted mice, we performed Ki67-staining to identify cells undergoing active
499 proliferation and found that this subset was highly proliferative compared to the single exposed
500 mice (Fig 6D and E). No differences were found in the frequency of proliferating Foxp3 negative
501 alveolar macrophages (Fig 6F and 6G). Therefore, upon subsequent exposures to $Cl_2$ Foxp3-
502 expressing alveolar macrophages preferentially proliferate. To confirm the protective role of
503 this subset of proliferating alveolar macrophage in adaptation, we adoptively transferred
504 alveolar macrophages isolated by cell sorting from adapted or naïve wild type mice or from

adapted Foxp3-RFP mice, into naïve mice that were subsequently exposed to $Cl_2$ (Fig 6H). We verified by flow cytometry that adapted $RFP^-$ and $RFP^+$ alveolar macrophages were negative and positive for Foxp3, respectively (Fig 6I), as well as by qPCR in $Foxp3^+$ versus $Foxp3^-$ alveolar macrophages isolated by cell sorting (Fig 6J). The expression of the Foxp3 transcript by the $Foxp3^+$ cells, sorted based on red fluorescence, was 5.9 times that of the expression by $Foxp3^-$ cells and statistically significant ($p = 0.014$). Both AHR and neutrophilia were significantly reduced only in mice that received adapted alveolar macrophages and this effect was completely abrogated in mice receiving adapted alveolar macrophages depleted of the Foxp3-expressing subset (Fig 6K-M). Therefore, adaptation to $Cl_2$ is mediated by a proliferative population of Foxp3-expressing alveolar macrophages.

**Differential gene expression between naïve and adapted alveolar macrophages**

To explore the expression profile of alveolar macrophages prior to and after adaptation, we performed a transcriptomic analysis of FACS-sorted alveolar macrophages from naïve and adapted mice (Fig 7A and Fig E7). We found 177 genes differentially expressed between adapted and naïve alveolar macrophages: 102 genes were up-regulated and 75 genes were down-regulated (Fig 7A). Among the 102 up-regulated genes, 20 had an FDR (False Discovery Rate) p-value ≤ 0.05 (Table E1). Interestingly, the expression profile revealed 3 upregulated genes (*Pla2g7*, *Ptgs1* and *Fads1*) linked to the synthesis of the anti-inflammatory and bronchodilator molecule $PGE_2$. Interestingly, the gene (*Thbs1*) encoding thrombospondin, which is required for TGF-β1 activation (42) was also substantially increased in expression. To further

characterize adapted alveolar macrophages, we assessed the expression of these highlighted genes in the population of $Foxp3^+$ and $Foxp3^-$ alveolar macrophages. The expression of *Thbs1* (Fig 7B) and *Ptgs1* (Fig 7C) was further increased in the $Foxp3^+$ alveolar macrophages (*Thbs1* being expressed 7-fold more in $Foxp3^+$ cells). These results suggest that the $Foxp3^+$ alveolar macrophages have distinguishing transcriptomic signatures that involve both the enzymes of prostaglandin $E_2$ synthesis and thrombospondin 1.

**Adaptation is incomplete in mice deficient in *Ptges***

$PGE_2$ has been described to induce Foxp3 in CD4 T cells (43). While three enzymes have been shown to independently generate $PGE_2$, microsomal prostaglandin E-synthase 1 (mPGES-1) is the dominant isoform for $PGE_2$ synthesis during inflammation involving macrophages (44). Thus we anticipated that $PGE_2$ synthesis was required to promote Foxp3 expression in alveolar macrophages. Initially, we found that *Ptges* (the gene for mPGES1) expression was increased in $Foxp3^+$ alveolar macrophages compared to $Foxp3^-$ macrophages derived from the adapted mice (Fig 8A), while the frequency of $Foxp3^+$ alveolar macrophages in *Ptges*-deficient mice exposed to repeated $Cl_2$ was significantly reduced (Fig 8B-C and Fig E6A-B). The amount of $PGE_2$ in the BAL of wild type mice was significantly increased after $Cl_2$ exposure, with a trend for further increase in adapted mice (Fig 8D). $PGE_2$ in the BAL of $Ptges^{-/-}$ mice was increased only after 1 exposure and trended towards decrease in adapted mice (Fig 8D). Interestingly, while neutrophilia, but not macrophage numbers, was significantly decreased in repeatedly $Cl_2$ exposed $Ptges^{-/-}$ mice (Fig 8F-G), there was diminished adaptation of AHR as reflected in

547 Resistance (Fig 8E), indicating a role for $PGE_2$ in a bronchoprotective effect on conducting
548 airways rather than an anti-inflammatory action. Adaptation in the H parameter that reflects
549 the dynamic stiffness of the peripheral lung compartment remained (data not shown),
550 suggesting distinct regulatory mechanisms in large versus small airways.
551
552 **Antibody neutralization of TGF-β reverses adaptation**
553 Since thrombospondin 1 has been described to be the main activator of latent TGF-β1 (42), and
554 TGF-β1 has been involved in the tolerogenic response (15), we addressed the possible role of
555 TGF-β1 in adaptation. Indeed, TGF-β levels were elevated in the adapted mice, but not the
556 singly exposed mice (Fig 8H). Antibody neutralization of TGF-β restored both AHR and
557 neutrophilia after repeated $Cl_2$ exposures compared to isotype control treatment (Fig 8I-K),
558 consistent with a possible role for TGF-β in adaptation. The level of TGF-β in the BAL fluid of
559 *Ptges*$^{-/-}$ mice was slightly but not significantly lower than in wild type mice following three $Cl_2$
560 exposures (Fig 8H).
561

ACCEPTED MANUSCRIPT

ACCEPTED MANUSCRIPT

## DISCUSSION

In the current study, we have studied the response of mice to repeated exposure to $Cl_2$ and have shown a rapid adaptation with a marked abrogation of inflammation and airway hyperresponsiveness to inhaled methacholine, the latter a key surrogate for asthma. The adaptation was still present at one month after initial exposures. Adaptation was not mediated by enhanced antioxidant responses but was dependent on Foxp3-expressing cells. However, *Rag1*$^{-/-}$ mice showed comparable adaptation to wild type mice excluding regulatory T cells as primary mediators of the adaptive process. Adoptive transfer of alveolar macrophages from repeatedly $Cl_2$ exposed mice restored the adapted phenotype, and depletion of the subpopulation of Foxp3$^{+}$ macrophages from those transferred abolished the inhibitory effects. Alveolar macrophages expressing Foxp3 further increased the expression of genes involved in both $PGE_2$ synthesis and TGF-β activation.

The $Cl_2$-exposed mouse has been used frequently to study mechanisms of irritant-induced asthma or acute lung injury following exposure to single high concentrations of $Cl_2$ (45, 46). A very high exposure is associated with tissue remodeling (47) and when the basal cell population is damaged, leads to an occlusive lesion of the lower trachea, analogous to bronchiolitis obliterans (48). However, after a single exposure to concentrations of $Cl_2$ up to 400 ppm, mice resolve the inflammation, repair epithelial damage, and lose AHR by three days post exposure (21). We were surprised by the extent of adaptation of mice to repeated exposures. Based on prior demonstrations of the efficacy of anti-oxidants treatments (23, 28, 46), we anticipated

583 that the attenuated response to $Cl_2$ would be linked to an upregulated endogenous anti-oxidant
584 response. However, the adaptation was not associated with an enhanced endogenous anti-
585 oxidant response and anti-oxidant molecules, glutathione and Nrf2-dependent proteins, were
586 comparable to unexposed mice. These observations are indicative of an upstream protective
587 mechanism likely related to the attenuated neutrophilia, which have an important role in the
588 development of AHR and oxidative stress after $Cl_2$-induced airway injury (10) and are
589 themselves a potent source of hypochlorite.
590
591 Pulmonary macrophages have immunosuppressive properties and may prevent AHR (38, 49). As
592 such these cells were a logical target for consideration. To examine if alveolar macrophages
593 were the mediators of airway adaptation to oxidative injury, we used two different strategies of
594 depletion. Both strategies resulted in substantial depletion of alveolar macrophages, leading to
595 abolition of airway adaptation. In mice repeatedly exposed to $Cl_2$ and treated with clodronate,
596 the neutrophilic inflammation was enhanced. Depletion of $CD11c^+$ cells in CD11c DTR mice by
597 treatment with diphtheria toxin provided the same extent of alveolar macrophage depletion as
598 clodronate and likewise reversed the apparent adaptation. The methacholine responsiveness of
599 unexposed and single $Cl_2$ exposed mice was not affected but only the response to repeated $Cl_2$
600 exposure of mice was enhanced such that there was an abolition of the adaptive response.
601 While peripheral blood neutrophilia is described following depletion of $CD11c^+$ cells with
602 diphtheria toxin (50), we have not found any effect on the BAL cellularity of the control group
603 nor an exacerbation of inflammation in the group exposed to $Cl_2$ once. We did however find

604 that $CD11c^+$ cell depletion also reduced dendritic cells in the lungs. Despite their being a small
605 fraction of $CD11c^+$ cells we cannot exclude a contribution of dendritic cells to the observed
606 findings.
607
608 That adaptation to $Cl_2$ is mediated by alveolar macrophages is supported by the results of the
609 adoptive transfer of these cells from $Cl_2$ exposed mice to naïve mice subsequently exposed to
610 $Cl_2$. Alveolar macrophages, sorted from BAL fluid of adapted mice, and administered
611 intratracheally, recapitulated the airway adaptation compared to alveolar macrophages sorted
612 from naïve mice. Adoptive transfer of naïve alveolar macrophages did not provide protection
613 against a single $Cl_2$ exposure nor did their depletion lead to AHR that exceeded mice that did
614 not undergo macrophage depletion. Thus, we conclude that the suppressive functions of
615 alveolar macrophages are triggered in response to a stimulus in order to restore a steady state,
616 suggesting here that alveolar macrophages need to be "educated" to offer the observed
617 protection. Given the rarity of dendritic cells in BAL fluid we are inclined to discount a role for
618 these cells in adaptation. However, many of the interventions employed to implicate alveolar
619 macrophages likely affected dendritic cell populations and thus we cannot exclude the
620 possibility that these cells were playing a role.
621
622 Previous studies have shown that $Foxp3^+$ Treg cells (15, 30-32) play an important role in
623 regulating pulmonary inflammation. However, these cells did not increase in the adapted state.
624 To test the effects of their depletion we administered diphtheria toxin to DEREG mice. Although

there was effective depletion of $CD4^+CD25^+Foxp3^+$ cells and reversal of the adaptation to repeated $Cl_2$ exposure following the diphtheria toxin, there was no loss of the adaptive response in *Rag1*$^{-/-}$ mice. These findings suggested that depletion of a Foxp3 expressing cell other than Tregs was responsible for our findings. ~~2~~$_2$However, it is possible that the adaptive response of *Rag1*$^{-/-}$ mice on repeated exposure to chlorine is not mediated by similar mechanisms to wild type mice and therefore the conclusion that Tregs are not important based on these observations requires verification.

Since Foxp3 and alveolar macrophages were both required for adaptation, we examined if Foxp3 was expressed in macrophages from adapted mice. Autofluorescence by macrophages has the potential to confound the results of flow cytometry. Cognizant of this problem we used a fluorochrome far from the autofluoresence spectrum of macrophages and observed that among the alveolar macrophages ($F4/80^+$ $CD11c^+$) approximately 5% of the cells were $Foxp3^+$ but only when harvested from adapted mice. RFP is co-expressed as an independent protein from Foxp3 in Foxp3-expressing cells in Foxp3-RFP mice, under the direction of an internal ribosomal entry site. Confirmation of a double positive Foxp3-expressing alveolar macrophage population ($F4/80^+CD11c^+RFP^{pos}$ and Foxp3-PE-$Cy7^+$) was demonstrated, increasing our confidence in the existence of this subset of Foxp3-expressing macrophages. Although the frequency of Foxp3-PE-$Cy7^+$ alveolar macrophages was modest, we also observed a two-fold shift to the right in the mean fluorescence intensity of the Foxp3-PE-Cy7 signal in all $RFP^{pos}$ compared to all $RFP^{neg}$ populations of alveolar macrophages. An attempt to confirm Foxp3

646 protein expression in isolated $RFP^+$ alveolar macrophages ($F4/80^+CD11c^+$) from the lungs of $Cl_2$-
647 adapted mice by Western blot was unsuccessful due to prohibitive cell numbers recovered
648 following a 1-hour incubation of digested lungs on tissue culture plates aimed at enriching
649 macrophage cell numbers.
650
651 Additional findings support the conclusion that a subset of macrophages indeed expresses
652 Foxp3. Diphtheria toxin treatment, as expected, depleted these cells in DEREG mice and
653 adapted alveolar macrophages identified as $Foxp3^+$ by expression of RFP in Foxp3-RFP mice and
654 subsequently sorted had higher levels of Foxp3 mRNA compared to $RFP^{neg}$ macrophages. On the
655 gene array comparing naïve and adapted alveolar macrophages, Foxp3 transcripts were 1.35
656 fold increased in adapted ones. This increase did not achieve statistical significance perhaps
657 because of the small sample size and inadequate statistical power, and the fact that we did not
658 isolate the pertinent 5% of $Foxp3^+$ macrophages. One limitation of our study in linking Foxp3
659 expression by macrophages to adaptation was the difficulty in transferring the same number of
660 $Foxp3^+$ alveolar macrophages as were transferred among the alveolar macrophages from
661 adapted mice. Adoptive transfer of solely $Foxp3^+$ macrophages would have required the
662 sacrifice of many adapted Foxp3-RFP mice. Thus, we chose to transfer adapted alveolar
663 macrophages depleted of the cells expressing Foxp3 and we confirmed that these alveolar
664 macrophages failed to recapitulate adaptation.
665

Gene candidates that may be linked to a protective role of alveolar macrophages during airway adaptation were identified by transcriptomic analysis. Among the 20 genes up-regulated in adapted alveolar macrophages with an FDR ≤ 0.05, 3 of them were linked to $PGE_2$ synthesis. $PGE_2$ was present in BAL in high concentrations following $Cl_2$ exposure, however we did not establish the source of the $PGE_2$. When mice were deficient in Ptges, Foxp3 expression was absent from alveolar macrophages, suggesting that $PGE_2$ may have a role in promoting Foxp3 expression. Following adaptation, $Foxp3^+$ cells further increased gene expression of the $PGE_2$ synthesis pathway suggesting a possible contribution of these cells to the BAL $PGE_2$ levels. However, $PGE_2$ alone did not explain entirely the adaptation process, so we next examined the possible role of TGF-β. Indeed, thrombospondin 1, which is the main activator of latent TGF-β, had the highest fold change in adapted alveolar macrophages and was increased further in the $Foxp3^+$ population. Using a neutralizing antibody to TGF-β, we demonstrated a reversal of the adaptation both from the standpoint of AHR and inflammation. In addition to the role of TGF-β in the repair process, it is possible that TGF-β acted as when secreted by Tregs to maintain suppressor function and Foxp3 expression in alveolar macrophages (51). Although our study demonstrated that $PGE_2$ and TGF-β are two potential mediators of adaptation, our evidence is consistent with this idea but not proven, since we have not shown that $Foxp3^+$ macrophages do indeed inhibit inflammation and AHR by these pathways. Furthermore, whether there is a cross-talk between these mediators requires further exploration. We did not find a reduced level of TGF-β in the BAL fluid of Ptges-deficient mice arguing against a transcriptional regulation of TGF-β by $PGE_2$.

687

688 In addition to genes involved in $PGE_2$ synthesis or TGF-β activation, some genes may be involved
689 in the resolution of inflammation, phagocytosis/efferocytosis or repair (Table E2). It is possible
690 that alveolar macrophages in adapted mice display an increased phagocytic capacity, which may
691 contribute to the control of neutrophilic inflammation. The gene array showed that alveolar
692 macrophages from adapted mice increased the expression of the scavenger receptor Msr1.
693 Thus, our results suggest that in addition to $PGE_2$ and TGF-β, the removal of oxidized lipids, as
694 well as the removal of damaged cells by phagocytosis, might be a significant element of airway
695 adaptation. Importantly, phagocytosis is crucial to remove cellular debris following $Cl_2$
696 exposure. Notably, a defect in phagocytosis has been observed in respiratory pathologies
697 including asthma (52, 53), chronic obstructive pulmonary disease (54), cystic fibrosis (55, 56)
698 and idiopathic pulmonary fibrosis (57) and has been invoked as a cause of sustained
699 inflammation. Adaptation after repeated ozone exposures has been described in asthmatic
700 subjects and an increase in alveolar macrophages was noted in association with adaptation (58).
701 Studies on mice exposed to ozone reproduced the adaptation of lung function parameters
702 observed in humans and highlight an important role of alveolar macrophages in that protection
703 by scavenging oxidized lipids (59).

704

705 Using a complex model of respiratory system mechanics (29), it was possible to demonstrate
706 that large and small airway contributed to AHR after $Cl_2$ inhalation, consistent with previous
707 published results. However, the attenuation of AHR mediated by $PGE_2$ was not uniform in all

lung compartments. The predominant effect was on resistance parameters, (Rrs, Rn and G) while adaptation of the peripheral lung compartment reflected in the tissue elastance (H) parameter was not affected by the absence of $PGE_2$ in the *Ptges* deficient mice. Although $PGE_2$ has been described to have both anti-inflammatory and bronchodilator properties (60, 61), our results suggest that $PGE_2$ acts mainly as a bronchoprotective agonist and its protective influence is predominantly with the conducting airway compartment of the lung. TGF-β in contrast was associated with adaptation in both central and peripheral airway compartments. While changes in Rn are more likely mediated by smooth muscle contraction, the peripheral airway response may also reflect other phenomena such as the formation of liquid bridges and enhanced surface tension, leading to airway closure.

In conclusion, after repeated oxidative stress-induced lung injury, resident alveolar macrophages seem to develop an enhanced protective function either through the inhibition of inflammation or possibility by the accelerated resolution by phagocytosis/efferocytosis. A subset of highly proliferative alveolar macrophages that are $Foxp3^+$ express mRNA for tolerogenic signaling pathways that may be required for preservation of lung function after oxidative injury. $PGE_2$ synthesis appears to be important for adaptation of airway dysfunction affecting the large conducting airways. It is plausible that TGF-β activation by upregulated thrombospondin occurs and when neutralized releases mechanisms that cause inflammation and airway hyperresponsiveness. Future studies should determine if human alveolar macrophages can express Foxp3 and if a defect of expression may be associated to airway

729 disease severity. Potentially, Foxp3 expression by alveolar macrophages might be used as a
730 biomarker of lung adaptation after injury and predict favorable prognosis from noxious insults
731 to the lung.
732

ACCEPTED MANUSCRIPT

ACCEPTED MANUSCRIPT

733 **ACKNOWLEDGEMENT:** We would like to thank the histopathology and immunophenotyping
734 platform of the RI-MUHC for their support as well as Genome Quebec. The authors thank G.N.
735 Kaufman for technical discussions.

736

ACCEPTED MANUSCRIPT

ACCEPTED MANUSCRIPT

## REFERENCES


1. Bowatte G, Lodge CJ, Knibbs LD, Lowe AJ, Erbas B, Dennekamp M, et al. Traffic-related air pollution exposure is associated with allergic sensitization, asthma, and poor lung function in middle age. The Journal of allergy and clinical immunology. 2016.
2. Saxon A, Diaz-Sanchez D. Air pollution and allergy: you are what you breathe. Nature immunology. 2005;6(3):223-6.
3. Clark KA, Karmaus WJ, Mohr LC, Cai B, Balte P, Gibson JJ, et al. Lung Function before and after a Large Chlorine Gas Release in Graniteville, South Carolina. Annals of the American Thoracic Society. 2016;13(3):356-63.
4. White CW, Martin JG. Chlorine gas inhalation: human clinical evidence of toxicity and experience in animal models. Proceedings of the American Thoracic Society. 2010;7(4):257-63.
5. Holguin F. Oxidative stress in airway diseases. Annals of the American Thoracic Society. 2013;10 Suppl:S150-7.
6. Lakey PS, Berkemeier T, Tong H, Arangio AM, Lucas K, Poschl U, et al. Chemical exposure-response relationship between air pollutants and reactive oxygen species in the human respiratory tract. Scientific reports. 2016;6:32916.
7. Sin DD, Wu L, Man SF. The relationship between reduced lung function and cardiovascular mortality: a population-based study and a systematic review of the literature. Chest. 2005;127(6):1952-9.
8. Grommes J, Soehnlein O. Contribution of neutrophils to acute lung injury. Molecular medicine (Cambridge, Mass). 2011;17(3-4):293-307.
9. Porto BN, Stein RT. Neutrophil Extracellular Traps in Pulmonary Diseases: Too Much of a Good Thing? Frontiers in immunology. 2016;7:311.
10. McGovern TK, Goldberger M, Allard B, Farahnak S, Hamamoto Y, O'Sullivan M, et al. Neutrophils mediate airway hyperresponsiveness after chlorine-induced airway injury in the mouse. American journal of respiratory cell and molecular biology. 2015;52(4):513-22.
11. Farrell BP, Kerr HD, Kulle TJ, Sauder LR, Young JL. Adaptation in human subjects to the effects of inhaled ozone after repeated exposure. The American review of respiratory disease. 1979;119(5):725-30.
12. Serhan CN, Savill J. Resolution of inflammation: the beginning programs the end. Nature immunology. 2005;6(12):1191-7.
13. Campbell DJ, Koch MA. Phenotypical and functional specialization of FOXP3+ regulatory T cells. Nature reviews Immunology. 2011;11(2):119-30.
14. Kearley J, Barker JE, Robinson DS, Lloyd CM. Resolution of airway inflammation and hyperreactivity after in vivo transfer of CD4+CD25+ regulatory T cells is interleukin 10 dependent. The Journal of experimental medicine. 2005;202(11):1539-47.
15. D'Alessio FR, Tsushima K, Aggarwal NR, West EE, Willett MH, Britos MF, et al. CD4+CD25+Foxp3+ Tregs resolve experimental lung injury in mice and are present in humans with acute lung injury. The Journal of clinical investigation. 2009;119(10):2898-913.
16. Korns D, Frasch SC, Fernandez-Boyanapalli R, Henson PM, Bratton DL. Modulation of macrophage efferocytosis in inflammation. Frontiers in immunology. 2011;2:57.

778 17. Ortega-Gomez A, Perretti M, Soehnlein O. Resolution of inflammation: an integrated
779 view. EMBO molecular medicine. 2013;5(5):661-74.
780 18. Allard B, Panariti A, Martin JG. Alveolar Macrophages in the Resolution of Inflammation,
781 Tissue Repair, and Tolerance to Infection. Frontiers in immunology. 2018;9:1777.
782 19. Hussell T, Bell TJ. Alveolar macrophages: plasticity in a tissue-specific context. Nature
783 reviews Immunology. 2014;14(2):81-93.
784 20. Degrossoli A, Muller A, Xie K, Schneider JF, Bader V, Winklhofer KF, et al. Neutrophil-
785 generated HOCl leads to non-specific thiol oxidation in phagocytized bacteria. eLife. 2018;7.
786 21. Martin JG, Campbell HR, Iijima H, Gautrin D, Malo JL, Eidelman DH, et al. Chlorine-
787 induced injury to the airways in mice. American journal of respiratory and critical care
788 medicine. 2003;168(5):568-74.
789 22. Itoh K, Chiba T, Takahashi S, Ishii T, Igarashi K, Katoh Y, et al. An Nrf2/small Maf
790 heterodimer mediates the induction of phase II detoxifying enzyme genes through antioxidant
791 response elements. Biochemical and biophysical research communications. 1997;236(2):313-
792 22.
793 23. McGovern T, Day BJ, White CW, Powell WS, Martin JG. AEOL10150: a novel therapeutic
794 for rescue treatment after toxic gas lung injury. Free radical biology & medicine.
795 2011;50(5):602-8.
796 24. Ano S, Panariti A, Allard B, O'Sullivan M, McGovern TK, Hamamoto Y, et al. Inflammation
797 and airway hyperresponsiveness after chlorine exposure are prolonged by Nrf2 deficiency in
798 mice. Free radical biology & medicine. 2017;102:1-15.
799 25. McGovern T, Goldberger M, Chen M, Allard B, Hamamoto Y, Kanaoka Y, et al. CysLT1
800 Receptor Is Protective against Oxidative Stress in a Model of Irritant-Induced Asthma. Journal of
801 immunology (Baltimore, Md : 1950). 2016.
802 26. Parmentier C, Leroy P, Wellman M, Nicolas A. Determination of cellular thiols and
803 glutathione-related enzyme activities: versatility of high-performance liquid chromatography-
804 spectrofluorimetric detection. Journal of chromatography B, Biomedical sciences and
805 applications. 1998;719(1-2):37-46.
806 27. Tung JW, Parks DR, Moore WA, Herzenberg LA, Herzenberg LA. New approaches to
807 fluorescence compensation and visualization of FACS data. Clinical immunology (Orlando, Fla).
808 2004;110(3):277-83.
809 28. McGovern TK, Powell WS, Day BJ, White CW, Govindaraju K, Karmouty-Quintana H, et
810 al. Dimethylthiourea protects against chlorine induced changes in airway function in a murine
811 model of irritant induced asthma. Respiratory research. 2010;11:138.
812 29. Bates JH. Pulmonary mechanics: a system identification perspective. Conference
813 proceedings : Annual International Conference of the IEEE Engineering in Medicine and Biology
814 Society IEEE Engineering in Medicine and Biology Society Annual Conference. 2009;2009:170-2.
815 30. Lewkowicz P, Lewkowicz N, Sasiak A, Tchorzewski H. Lipopolysaccharide-activated
816 CD4+CD25+ T regulatory cells inhibit neutrophil function and promote their apoptosis and
817 death. Journal of immunology (Baltimore, Md : 1950). 2006;177(10):7155-63.

818 31. Lewkowicz N, Klink M, Mycko MP, Lewkowicz P. Neutrophil--CD4+CD25+ T regulatory
819 cell interactions: a possible new mechanism of infectious tolerance. Immunobiology.
820 2013;218(4):455-64.
821 32. Richards H, Williams A, Jones E, Hindley J, Godkin A, Simon AK, et al. Novel role of
822 regulatory T cells in limiting early neutrophil responses in skin. Immunology. 2010;131(4):583-
823 92.
824 33. Gagliani N, Amezcua Vesely MC, Iseppon A, Brockmann L, Xu H, Palm NW, et al. Th17
825 cells transdifferentiate into regulatory T cells during resolution of inflammation. Nature.
826 2015;523(7559):221-5.
827 34. Pyle CJ, Uwadiae FI, Swieboda DP, Harker JA. Early IL-6 signalling promotes IL-27
828 dependent maturation of regulatory T cells in the lungs and resolution of viral
829 immunopathology. PLoS pathogens. 2017;13(9):e1006640.
830 35. Buch T, Heppner FL, Tertilt C, Heinen TJ, Kremer M, Wunderlich FT, et al. A Cre-inducible
831 diphtheria toxin receptor mediates cell lineage ablation after toxin administration. Nature
832 methods. 2005;2(6):419-26.
833 36. Lahl K, Loddenkemper C, Drouin C, Freyer J, Arnason J, Eberl G, et al. Selective depletion
834 of Foxp3+ regulatory T cells induces a scurfy-like disease. The Journal of experimental medicine.
835 2007;204(1):57-63.
836 37. Mombaerts P, Iacomini J, Johnson RS, Herrup K, Tonegawa S, Papaioannou VE. RAG-1-
837 deficient mice have no mature B and T lymphocytes. Cell. 1992;68(5):869-77.
838 38. Careau E, Bissonnette EY. Adoptive transfer of alveolar macrophages abrogates
839 bronchial hyperresponsiveness. American journal of respiratory cell and molecular biology.
840 2004;31(1):22-7.
841 39. Guilliams M, De Kleer I, Henri S, Post S, Vanhoutte L, De Prijck S, et al. Alveolar
842 macrophages develop from fetal monocytes that differentiate into long-lived cells in the first
843 week of life via GM-CSF. The Journal of experimental medicine. 2013;210(10):1977-92.
844 40. Boring L, Gosling J, Chensue SW, Kunkel SL, Farese RV, Jr., Broxmeyer HE, et al. Impaired
845 monocyte migration and reduced type 1 (Th1) cytokine responses in C-C chemokine receptor 2
846 knockout mice. The Journal of clinical investigation. 1997;100(10):2552-61.
847 41. Devaud C, Darcy PK, Kershaw MH. Foxp3 expression in T regulatory cells and other cell
848 lineages. Cancer immunology, immunotherapy : CII. 2014;63(9):869-76.
849 42. Crawford SE, Stellmach V, Murphy-Ullrich JE, Ribeiro SM, Lawler J, Hynes RO, et al.
850 Thrombospondin-1 is a major activator of TGF-beta1 in vivo. Cell. 1998;93(7):1159-70.
851 43. Baratelli F, Lin Y, Zhu L, Yang SC, Heuze-Vourc'h N, Zeng G, et al. Prostaglandin E2
852 induces FOXP3 gene expression and T regulatory cell function in human CD4+ T cells. Journal of
853 immunology (Baltimore, Md : 1950). 2005;175(3):1483-90.
854 44. Hara S, Kamei D, Sasaki Y, Tanemoto A, Nakatani Y, Murakami M. Prostaglandin E
855 synthases: Understanding their pathophysiological roles through mouse genetic models.
856 Biochimie. 2010;92(6):651-9.
857 45. Hoyle GW, Svendsen ER. Persistent effects of chlorine inhalation on respiratory health.
858 Annals of the New York Academy of Sciences. 2016.

859 46. Zarogiannis SG, Jurkuvenaite A, Fernandez S, Doran SF, Yadav AK, Squadrito GL, et al.
860 Ascorbate and deferoxamine administration after chlorine exposure decrease mortality and
861 lung injury in mice. American journal of respiratory cell and molecular biology. 2011;45(2):386-
862 92.
863 47. Tuck SA, Ramos-Barbon D, Campbell H, McGovern T, Karmouty-Quintana H, Martin JG.
864 Time course of airway remodelling after an acute chlorine gas exposure in mice. Respiratory
865 research. 2008;9:61.
866 48. O'Koren EG, Hogan BL, Gunn MD. Loss of basal cells precedes bronchiolitis obliterans-
867 like pathological changes in a murine model of chlorine gas inhalation. American journal of
868 respiratory cell and molecular biology. 2013;49(5):788-97.
869 49. Soroosh P, Doherty TA, Duan W, Mehta AK, Choi H, Adams YF, et al. Lung-resident tissue
870 macrophages generate Foxp3+ regulatory T cells and promote airway tolerance. The Journal of
871 experimental medicine. 2013;210(4):775-88.
872 50. Tittel AP, Heuser C, Ohliger C, Llanto C, Yona S, Hammerling GJ, et al. Functionally
873 relevant neutrophilia in CD11c diphtheria toxin receptor transgenic mice. Nature methods.
874 2012;9(4):385-90.
875 51. Marie JC, Letterio JJ, Gavin M, Rudensky AY. TGF-beta1 maintains suppressor function
876 and Foxp3 expression in CD4+CD25+ regulatory T cells. The Journal of experimental medicine.
877 2005;201(7):1061-7.
878 52. Huynh ML, Malcolm KC, Kotaru C, Tilstra JA, Westcott JY, Fadok VA, et al. Defective
879 apoptotic cell phagocytosis attenuates prostaglandin E2 and 15-hydroxyeicosatetraenoic acid in
880 severe asthma alveolar macrophages. American journal of respiratory and critical care
881 medicine. 2005;172(8):972-9.
882 53. Simpson JL, Gibson PG, Yang IA, Upham J, James A, Reynolds PN, et al. Impaired
883 macrophage phagocytosis in non-eosinophilic asthma. Clinical and experimental allergy : journal
884 of the British Society for Allergy and Clinical Immunology. 2013;43(1):29-35.
885 54. Hodge S, Hodge G, Scicchitano R, Reynolds PN, Holmes M. Alveolar macrophages from
886 subjects with chronic obstructive pulmonary disease are deficient in their ability to phagocytose
887 apoptotic airway epithelial cells. Immunology and cell biology. 2003;81(4):289-96.
888 55. McCaslin CA, Petrusca DN, Poirier C, Serban KA, Anderson GG, Petrache I. Impact of
889 alginate-producing Pseudomonas aeruginosa on alveolar macrophage apoptotic cell clearance.
890 Journal of cystic fibrosis : official journal of the European Cystic Fibrosis Society. 2015;14(1):70-
891 7.
892 56. Vandivier RW, Richens TR, Horstmann SA, deCathelineau AM, Ghosh M, Reynolds SD, et
893 al. Dysfunctional cystic fibrosis transmembrane conductance regulator inhibits phagocytosis of
894 apoptotic cells with proinflammatory consequences. American journal of physiology Lung
895 cellular and molecular physiology. 2009;297(4):L677-86.
896 57. Morimoto K, Janssen WJ, Terada M. Defective efferocytosis by alveolar macrophages in
897 IPF patients. Respiratory medicine. 2012;106(12):1800-3.
898 58. Arjomandi M, Witten A, Abbritti E, Reintjes K, Schmidlin I, Zhai W, et al. Repeated
899 exposure to ozone increases alveolar macrophage recruitment into asthmatic airways.
900 American journal of respiratory and critical care medicine. 2005;172(4):427-32.

59. Dahl M, Bauer AK, Arredouani M, Soininen R, Tryggvason K, Kleeberger SR, et al. Protection against inhaled oxidants through scavenging of oxidized lipids by macrophage receptors MARCO and SR-AI/II. The Journal of clinical investigation. 2007;117(3):757-64.
60. Ivanova V, Garbuzenko OB, Reuhl KR, Reimer DC, Pozharov VP, Minko T. Inhalation treatment of pulmonary fibrosis by liposomal prostaglandin E2. European journal of pharmaceutics and biopharmaceutics : official journal of Arbeitsgemeinschaft fur Pharmazeutische Verfahrenstechnik eV. 2013;84(2):335-44.
61. Martin JG, Suzuki M, Maghni K, Pantano R, Ramos-Barbon D, Ihaku D, et al. The immunomodulatory actions of prostaglandin E2 on allergic airway responses in the rat. Journal of immunology (Baltimore, Md : 1950). 2002;169(7):3963-9.

ACCEPTED MANUSCRIPT

912 **Figure legends**

913 **FIG 1. Mice develop a rapid lung function adaptation to repeated oxidative injury**. (**A**) Mice
914 were unexposed (Un) or nose only exposed once or three times at 84h intervals to $Cl_2$ gas for 5
915 minutes ($Cl_2$ x1 and $Cl_2$ x3 respectively). Lung function and inflammation were assessed 24h
916 after the last $Cl_2$ exposure. (**B**) Airway responsiveness to inhaled methacholine (Resistance) was
917 measured in C57BL/6 wild type mice (n=8/group pooled from 3 independent experiments).
918 **P<0.01, ***P<0.001 for $Cl_2$ x1 versus $Cl_2$ x3 and $^{###}$P< 0.001 for $Cl_2$ x1 versus Un (two-way
919 ANOVA). (**C**) Macrophages and (**D**) neutrophils in BAL fluid (n=8/group pooled from 3
920 independent experiments). *P<0.05, **P<0.01, ***P<0.001 (one-way ANOVA). (**E**) Absolute
921 number of cells in the airways. (**F**) Representative flow cytometry plots of unexposed, $Cl_2$ x1, or
922 $Cl_2$ x3 exposed airways. Neutrophils are considered viable $Ly6G^+$ cells, while macrophages are
923 viable $F4/80^+$ cells. Numbers in proximity to gates represent cells as a percentage of single
924 viable cells. Whole cell counts of (**G**) macrophages and (**H**) neutrophils based upon the flow
925 cytometry gating shown in (**F**) (n=4/group). *P<0.05, **P<0.01, ***P<0.001 (one-way ANOVA).
926 Data are mean ± 1SEM.

927 **FIG 2. Histological integrity of airway epithelial cells.** (**A**) Representative staining of apoptotic
928 (TUNEL) airway epithelial cells as quantified in (**C**) and (**B**) proliferating (PCNA) airway epithelial
929 cells (bar scale=100µm) as quantified in (**D**) (n=5/group). *P<0.05, ***P<0.001 (one-way
930 ANOVA). Data are mean ± 1SEM.

931

**FIG 3. Airway adaptation is independent of the anti-oxidant response**. (**A**) Reduced glutathione, (**B**) oxidized glutathione and (**C**) glutathione ratio in the bronchoalveolar lavage of exposed or unexposed mice (n=5-6 BALB/c WT/group). *P<0.05 (one-way ANOVA). (**D**) Responsiveness to inhaled methacholine (Resistance) was measured in *Nrf2*$^{-/-}$ mice (n=5-6/group pooled from 3 independent experiments). *P<0.05, ***P<0.001 for $Cl_2$ x1 versus $Cl_2$ x3 and $^{###}$P< 0.001 for $Cl_2$ x1 versus Un (two-way ANOVA). Absolute number of macrophages (**E**) and neutrophils (**F**) from bronchoalveolar lavage of *Nrf2*$^{-/-}$ mice (n=5-6/group pooled from 3 independent experiments). ***P<0.001 (two-way ANOVA). Data are mean ± 1SEM.

**FIG 4. Airway adaptation is dependent on Foxp3 expressing cells but not on regulatory T cells**. (**A**) Representative flow cytometry plots (left panels) showing extent of depletion of Foxp3-expressing regulatory T cells (single viable $CD4^+$ $CD25^+$ cells) following diphtheria toxin administration in DEREG mice, with frequencies quantified (right panel) (n=3-5 DEREG/group). *P<0.05 and $^{###}$P< 0.001 compare $Cl_2$ x3 + diphtheria toxin treatment to Un, $Cl_2$ x1 and $Cl_2$ x3 non-treated (one-way ANOVA). (**B**) Responsiveness to inhaled methacholine (Resistance) was measured in DEREG mice, with all groups treated with diphtheria toxin (n=4-5/group pooled from 2 independent experiments). ***P<0.001 for $Cl_2$ x3 versus Un and $^{###}$P< 0.001 for $Cl_2$ x1 versus Un (two-way ANOVA). (**C**) Absolute number of macrophages and (**D**) neutrophils from bronchoalveolar lavage of DEREG mice treated with diphtheria toxin (n=4-5/group from 2 independent experiments). **P<0.01 (one-way ANOVA). (**E**) Responsiveness to inhaled methacholine for *Rag1*$^{-/-}$ mice (n=5-6/group pooled from 3 independent experiments).

953 ***P<0.001 for $Cl_2$ x1 versus $Cl_2$ x3 and $^{###}$P< 0.001 for $Cl_2$ x1 versus Un (two-way ANOVA). (**F**)
954 Absolute number of macrophages and (**G**) neutrophils from bronchoalveolar lavage of *Rag1*$^{-/-}$
955 mice (n=5-6/group pooled from 3 independent experiments). *P<0.05, **P<0.01, ***P<0.001
956 (one-way ANOVA). Data are mean ± 1SEM.
957
958 **FIG 5. Airway adaptation is dependent on resident alveolar macrophages.** (**A**) Resistance of
959 the airways from CD11c DTR mice treated with diphtheria toxin in all groups to deplete alveolar
960 macrophages (n=4-5/group pooled from 3 independent experiments). ***P<0.001 for $Cl_2$ x3
961 versus Un and $^{##}$P<0.01, $^{###}$P< 0.001 for $Cl_2$ x1 and Un (two-way ANOVA). (**B**) Absolute number
962 of macrophages and (**C**) neutrophils from bronchoalveolar lavage of CD11c DTR mice treated
963 with diphtheria toxin (n=4-6/group pooled from 3 independent experiments) *P<0.05 (one-way
964 ANOVA). (**D**) Responsiveness to inhaled methacholine was measured in mice treated with
965 Clodrosome® to deplete alveolar macrophages or with the control Liposome (n=5-6/group
966 pooled from 3 independent experiments). *P<0.05, **P<0.01, ***P<0.001 for $Cl_2$ x3 +
967 Clodrosome® versus $Cl_2$ x3 + Liposome and $^{###}$P< 0.001 for $Cl_2$ x3 + Clodrosome® versus Un +
968 Clodrosome® (two-way ANOVA). (**E**) Absolute number of macrophages and (**F**) neutrophils from
969 bronchoalveolar lavage of mice treated with Clodrosome® or Liposome by Cytospin (n=5-
970 6/group pooled from 3 independent experiments). *P<0.05, **P<0.01, ***P<0.001 (one-way
971 ANOVA). (**G**) Responsiveness to inhaled methacholine for *Ccr2*$^{-/-}$ mice (n=4/group pooled from 2
972 independent experiments). ***P<0.001 for $Cl_2$ x1 versus $Cl_2$ x3 and $^{###}$P< 0.001 for $Cl_2$ x1 versus
973 Un (two-way ANOVA). (**H**) Total cell counts following 0, 1, or 3 exposures to $Cl_2$ in the

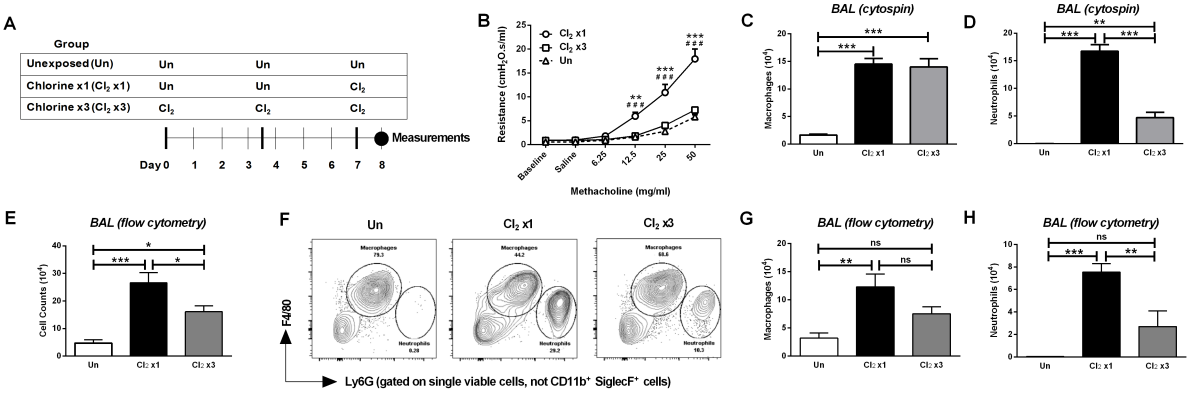
974 bronchoalveolar lavage of *Ccr2*$^{-/-}$ mice and levels of (**I**) macrophages and (**J**) neutrophils by
975 cytospin. (**K**) Representative flow cytometry plots showing the proportion of alveolar versus
976 recruited macrophages in the airways of exposed mice. The gating strategy exclude CD11b$^{+}$
977 SiglecF$^{+}$ cells to ensure that the alveolar macrophages are not contaminated by eosinophils.
978 Numbers in proximity to the gate indicate the percentage within that gate of total single viable
979 cells as quantified as a frequency in (**L** and **N**) or total number (**M** and **O**) for alveolar or
980 recruited macrophages (n=4/group from 2 independent experiments). *P<0.05, **P<0.01,
981 ***P<0.001 (one-way ANOVA). Data are mean ± 1SEM.
982
983 **FIG 6. Foxp3$^{+}$ alveolar macrophages from adapted mice recapitulate airway adaptation.** (**A**)
984 Representative flow cytometry plots of Foxp3-RFP$^{+}$ alveolar macrophages and quantification
985 (n=4/group). *P<0.05 (Mann-Whitney U test). (**B**) Quantification of Foxp3 expression in alveolar
986 macrophages (viable F4/80$^{+}$ CD11c$^{+}$ cells) in DEREG mice untreated or treated with diphtheria
987 toxin (right side) (n=3-5 DEREG/group). **P<0.01, ***P<0.001 (one-way ANOVA). (**C**) Flow
988 cytometry plot of Foxp3-RFP expressed in alveolar macrophages (pre-gated on viable, F4/80$^{+}$
989 CD11c$^{+}$ cells) from lungs of $Cl_2$x3-exposed mice following macrophage enrichment (>20 pooled
990 lungs). Arrows indicate plots assessing Foxp3-PE-Cy7 expression in Foxp3-RFP$^{pos}$ and Foxp3-
991 RFP$^{neg}$ alveolar macrophages. (**D**) Representative flow cytometry plots and (**E**) quantification of
992 proliferating (Ki67$^{hi}$) Foxp3$^{+}$ alveolar macrophages. (**F**) Representative flow cytometry plots and
993 (**G**) quantification of proliferating (Ki67$^{hi}$) Foxp3$^{-}$ alveolar macrophages. *P<0.05 (Mann-
994 Whitney U test for D and F). (**H**) Schema of the adoptive transfer procedure; sorted alveolar

995 macrophages from naïve or adapted mice were transferred intratracheally into naïve mice.
996 Foxp3-RFP mice were used to transfer Foxp3$^-$ alveolar macrophages from adapted mice. (**I**) Flow
997 cytometry and (**J**) qPCR were used to confirm RFP$^-$ and RFP$^+$ were negative and positive for
998 Foxp3 respectively (n=4/group). *P=0.0143 (Mann-Whitney U test). (**K**) Responsiveness to
999 inhaled methacholine in mice receiving naïve, total adapted, or Foxp3$^-$ adapted alveolar
1000 macrophages (n=5-8/group pooled from 2 independent experiments). ***P<0.001 for adapted
1001 AMs treated mice versus adapted AMs Foxp3$^-$ treated mice and $^{\#\#}$P<0.01, $^{\#\#\#}$P< 0.001 for
1002 adapted AMs treated mice versus naïve AMs treated mice (two-way ANOVA). (**L**) Absolute
1003 number of macrophages and (**M**) neutrophils from the bronchoalveolar lavage of mice (n=5-
1004 8/group pooled from 2 independent experiments). *P<0.05 (one-way ANOVA). Data are mean ±
1005 1SEM.
1006
1007 **FIG 7. Sorted alveolar macrophages from adapted mice exhibit a distinct gene expression.** (**A**)
1008 Volcano plot showing the 75 downregulated genes (fold change ≤ -2 on the left side) and the
1009 102 upregulated genes (fold change ≥ +2 on the right side) in adapted compared to naïve
1010 alveolar macrophages (crosses in bold are the 20 upregulated genes with a false discovery rate
1011 ≤ 0.05). (**B**) qPCR of *Thbs1* and (**C**) *Ptgs1* in Foxp3$^+$ versus Foxp3$^-$ adapted alveolar macrophages
1012 (n=4/group). *P<0.05 (Mann-Whitney U test). Data are mean ± 1SEM.
1013
1014 **FIG 8. Airway adaptation is dependent on $PGE_2$ and TGF-β.** (**A**) qPCR of *Ptges* in Foxp3$^+$ versus
1015 Foxp3$^-$ adapted alveolar macrophages (n=4/group). *P<0.05 (Mann-Whitney U test). (**B**)

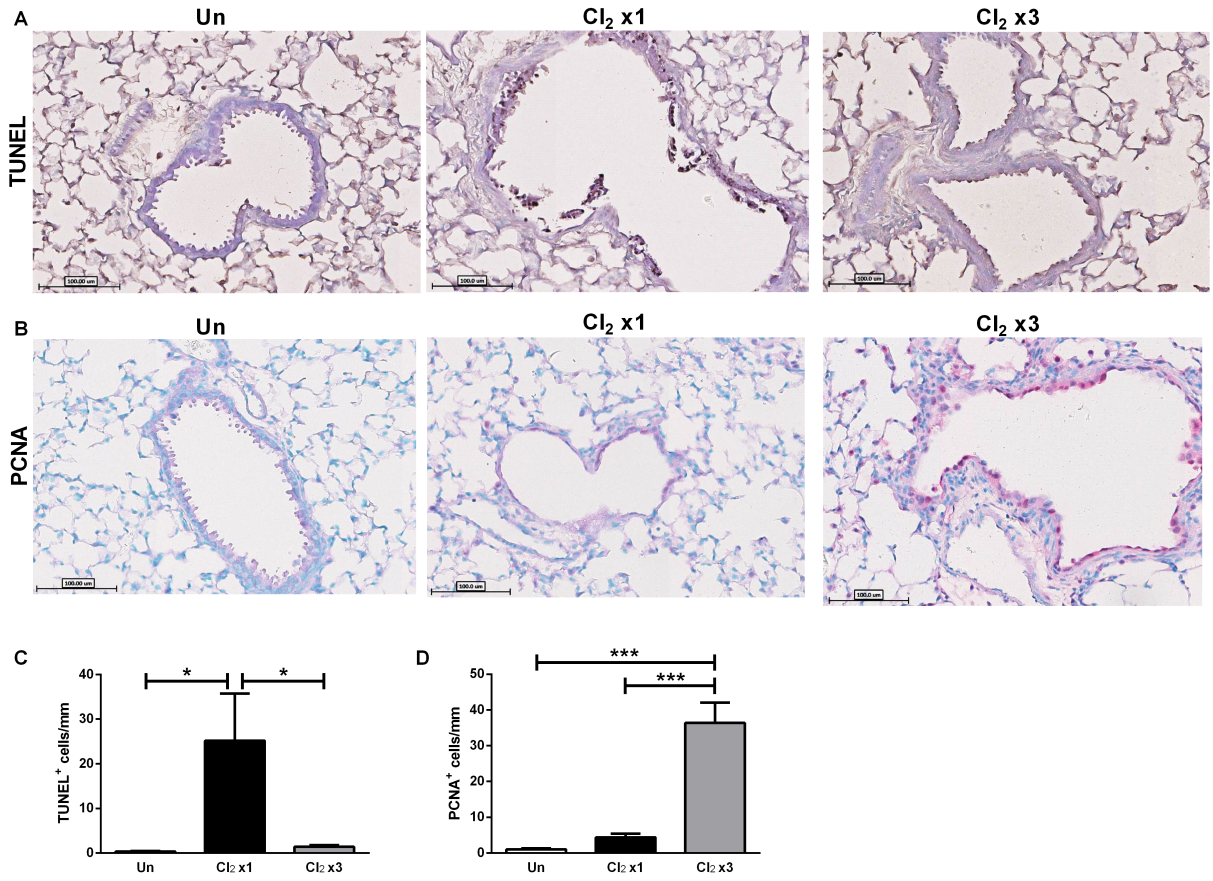
Representative flow cytometry plots and (**C**) quantification of Foxp3 expression in alveolar macrophages (viable F4/80$^{+}$ CD11c$^{+}$) from wild type or *Ptges*$^{-/-}$ mice after 3 repeated $Cl_2$ exposures (n=6-7/group pooled from 2 independent experiments). **P<0.01 (Mann-Whitney U test). (**D**) $PGE_2$ ELISA from bronchoalveolar lavage (n=7-8/group in wild type; n=5-6/group in *Ptges*$^{-/-}$). *P<0.05, **P<0.01, (one-way ANOVA). (**E**) Responsiveness to inhaled methacholine of *Ptges*$^{-/-}$ mice (n=5-6/group pooled from 2 independent experiments). **P<0.01, ***P<0.001 for $Cl_2$ x3 versus Un and $^{\#}$P<0.05, $^{\#\#\#}$P< 0.001 for $Cl_2$ x1 and Un (two-way ANOVA). (**F**) Absolute number of macrophages and (**G**) neutrophils from bronchoalveolar lavage of *Ptges*$^{-/-}$ mice (n=5-6/group pooled from 2 independent experiments). **P<0.01, ***P<0.001 (one-way ANOVA). (**H**) TGF-β ELISA from bronchoalveolar lavage (n=7-8/group in wild type; n=5-6/group in *Ptges*$^{-/-}$). *P<0.05, (one-way ANOVA). (**I**) Responsiveness to inhaled methacholine of wild type mice after repeated $Cl_2$ exposures treated with neutralizing anti-TGF-β antibody or isotype control (n=5/group). ***P<0.001 (two-way ANOVA). (**J**) Absolute number of macrophages and (**K**) neutrophils from bronchoalveolar lavage of wild type mice after repeated $Cl_2$ exposures treated with neutralizing anti-TGF-β antibody or isotype control (n=5/group). *P<0.05 (Mann-Whitney U test). Data are mean ± 1SEM.

ACCEPTED MANUSCRIPT

ACCEPTED MANUSCRIPT

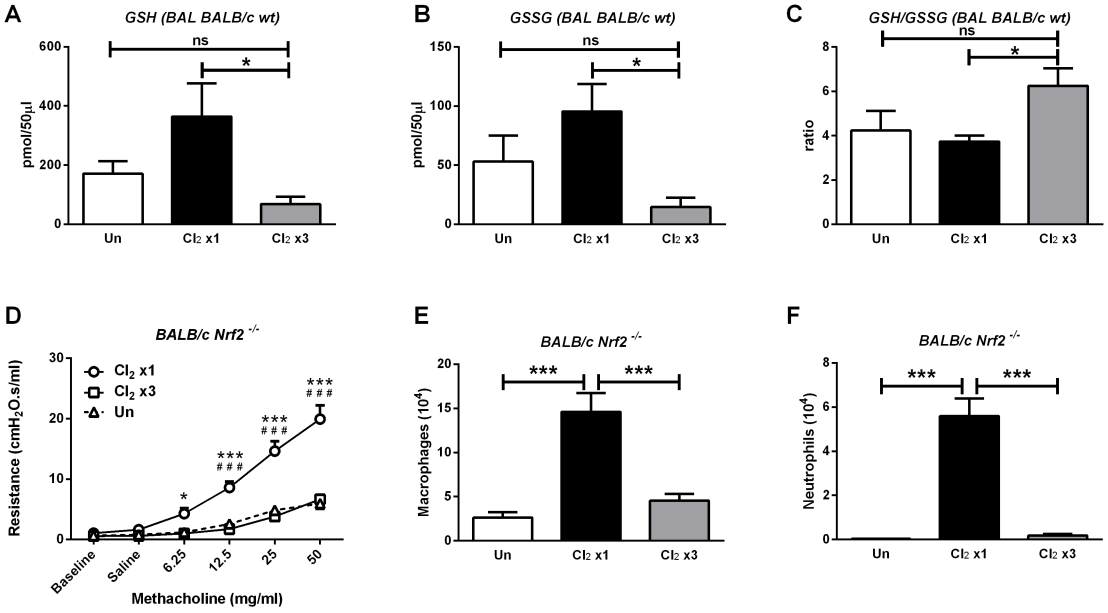



ACCEPTED MANUSCRIPT

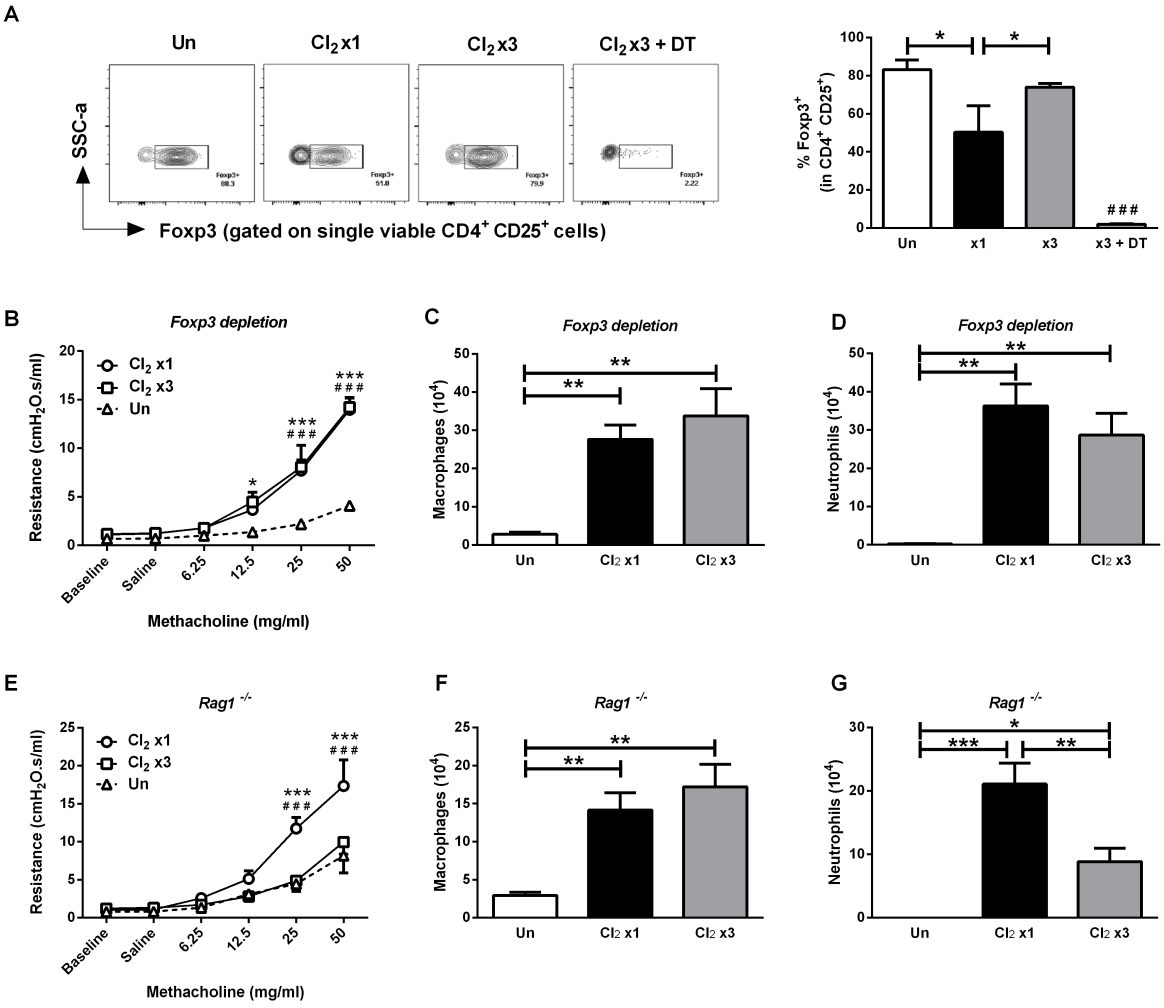

A
Un
Cl2 x1
Cl2 x3
TUNEL
B
Un
Cl2 x1
Cl2 x3
PCNA
C
TUNEL+ cells/mm
40
30
20
10
0
*
*
Un
Cl2 x1
Cl2 x3
D
PCNA+ cells/mm
50
40
30
20
10
0
***
***
Un
Cl2 x1
Cl2 x3

ACCEPTED

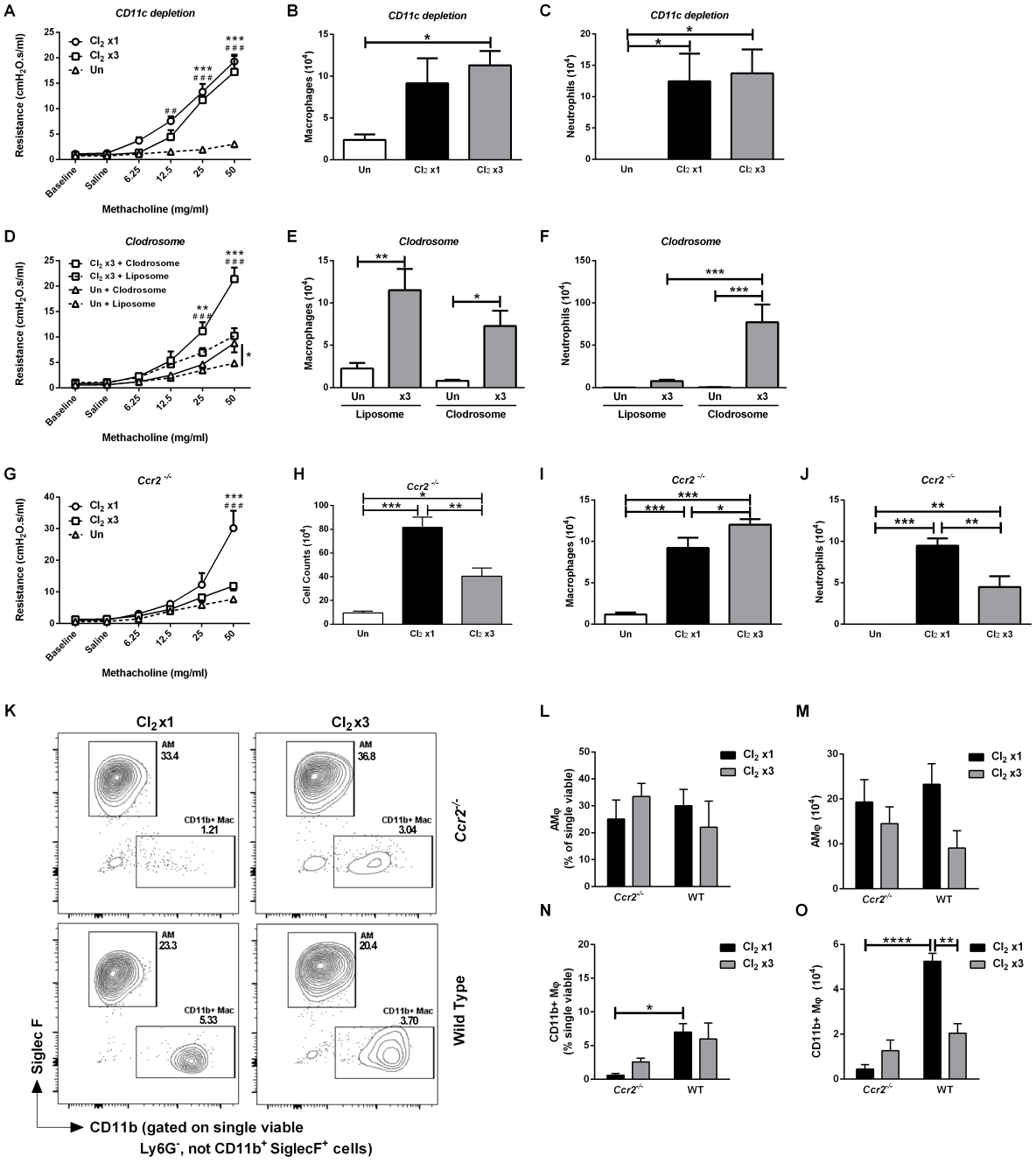
ACCEPTED MANUSCRIPT

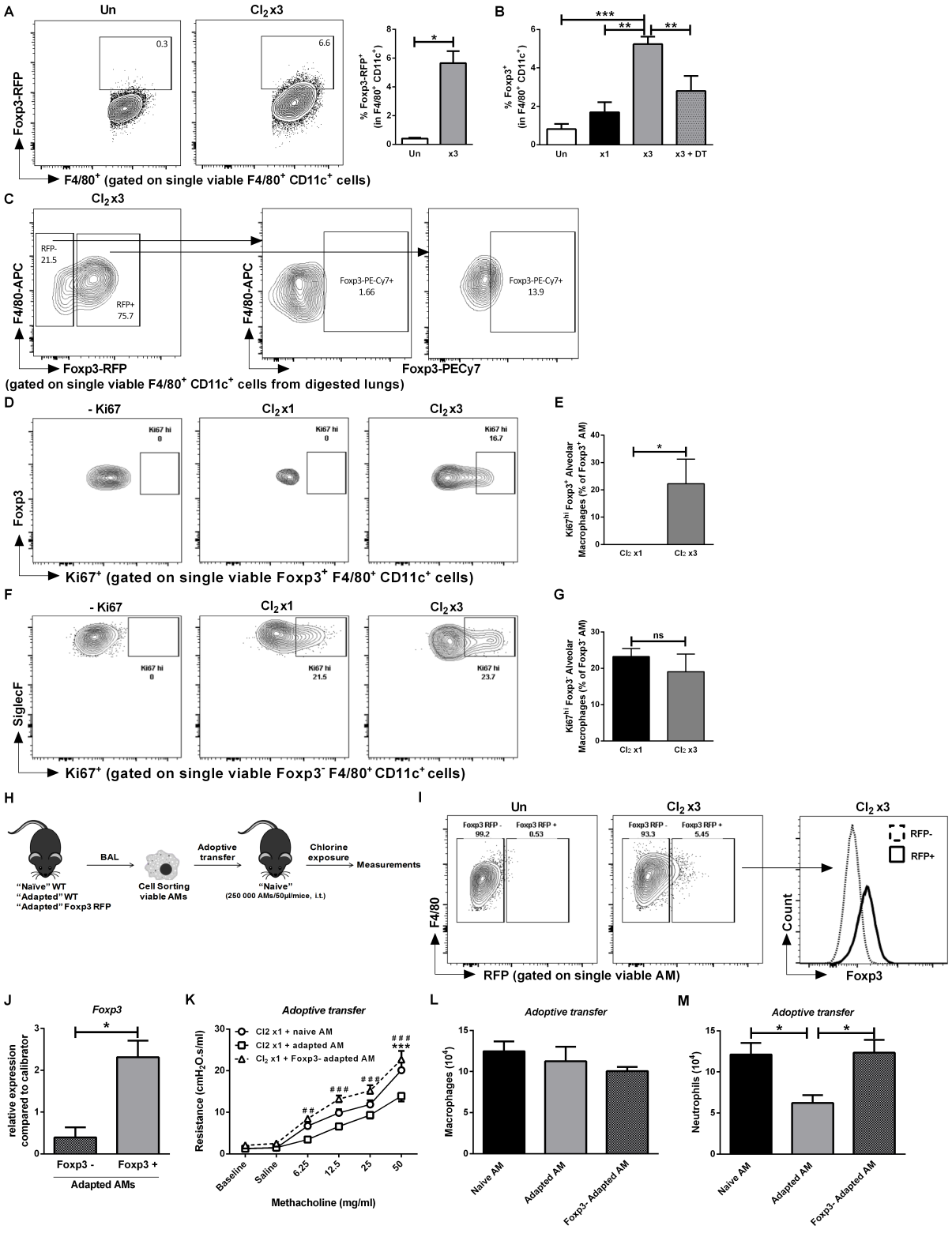


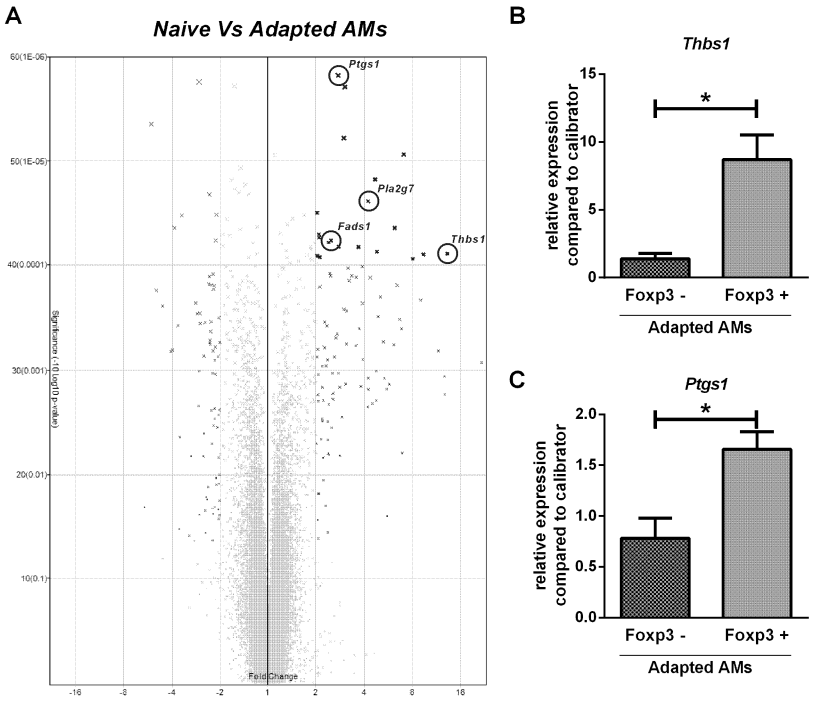

ACCEPTED MAN


A
Un
Cl2x1
Cl2x3
Cl2x3 + DT
SSC-a
Foxp3 (gated on single viable CD4+ CD25+ cells)
% Foxp3+ (in CD4+ CD25+)
Un
x1
x3
x3 + DT
B
Foxp3 depletion
Cl2 x1
Cl2 x3
Un
Resistance (cmH2O.s/ml)
Baseline
Saline
6.25
12.5
25
50
Methacholine (mg/ml)
C
Foxp3 depletion
Macrophages (10^4)
D
Foxp3 depletion
Neutrophils (10^4)
E
Rag1 -/-
Resistance (cmH2O.s/ml)
Methacholine (mg/ml)
F
Rag1 -/-
Macrophages (10^4)
G
Rag1 -/-
Neutrophils (10^4)

ACCEPTED MANUSCRIPT

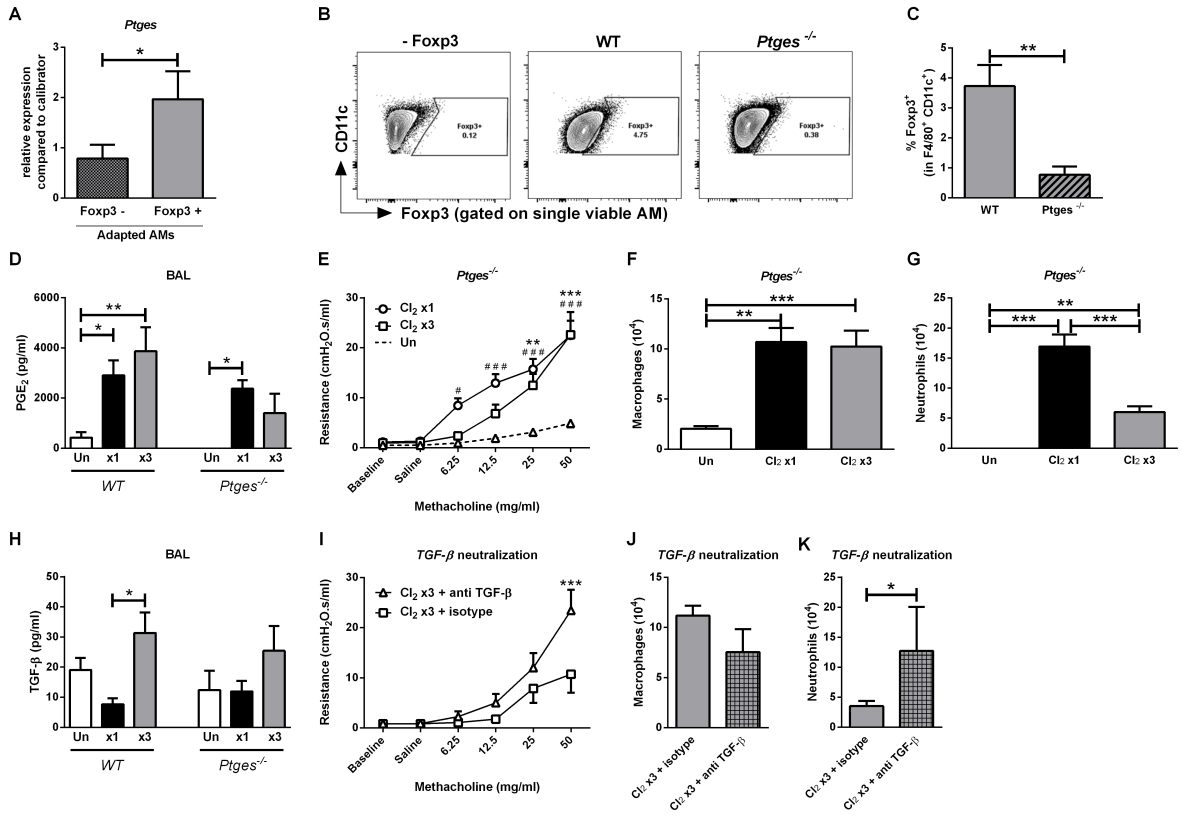



A
Un
Cl2x3
0.3
6.6
Foxp3-RFP
F4/80+ (gated on single viable F4/80+ CD11c+ cells)
% Foxp3-RFP+ (in F4/80+ CD11c+)
Un
x3
B
% Foxp3+ (in F4/80+ CD11c+)
Un
x1
x3
x3 + DT
C
Cl2x3
RFP- 21.5
RFP+ 75.7
F4/80-APC
Foxp3-RFP
Foxp3-PE-Cy7+ 1.66
Foxp3-PE-Cy7+ 13.9
Foxp3-PECy7
(gated on single viable F4/80+ CD11c+ cells from digested lungs)
D
- Ki67
Cl2x1
Cl2x3
Ki67 hi 0
Ki67 hi 16.7
Foxp3
Ki67+ (gated on single viable Foxp3+ F4/80+ CD11c+ cells)
E
Ki67hi Foxp3+ Alveolar Macrophages (% of Foxp3+ AM)
Cl2 x1
Cl2 x3
F
- Ki67
Cl2x1
Cl2x3
Ki67 hi 0
Ki67 hi 21.5
Ki67 hi 23.7
SiglecF
Ki67+ (gated on single viable Foxp3- F4/80+ CD11c+ cells)
G
ns
Ki67hi Foxp3- Alveolar Macrophages (% of Foxp3- AM)
Cl2 x1
Cl2 x3
H
"Naïve" WT
"Adapted" WT
"Adapted" Foxp3 RFP
BAL
Cell Sorting viable AMs
Adoptive transfer
"Naive" (250 000 AMs/50µl/mice, i.t.)
Chlorine exposure
Measurements
I
Un
Cl2 x3
Cl2 x3
Foxp3 RFP - 99.2
Foxp3 RFP + 0.53
Foxp3 RFP - 93.3
Foxp3 RFP + 5.45
RFP-
RFP+
F4/80
RFP (gated on single viable AM)
Count
Foxp3
J
Foxp3
relative expression compared to calibrator
Foxp3 -
Foxp3 +
Adapted AMs
K
Adoptive transfer
Cl2 x1 + naive AM
Cl2 x1 + adapted AM
Cl2 x1 + Foxp3- adapted AM
Resistance (cmH2O.s/ml)
Baseline
Saline
6.25
12.5
25
50
Methacholine (mg/ml)
L
Adoptive transfer
Macrophages (10^4)
Naive AM
Adapted AM
Foxp3- Adapted AM
M
Adoptive transfer
Neutrophils (10^4)
Naive AM
Adapted AM
Foxp3- Adapted AM




ACCEPTED MANUSCRIPT

ACCEPTED MANUSCRIPT



ACCEPTED MANUSCRIPT

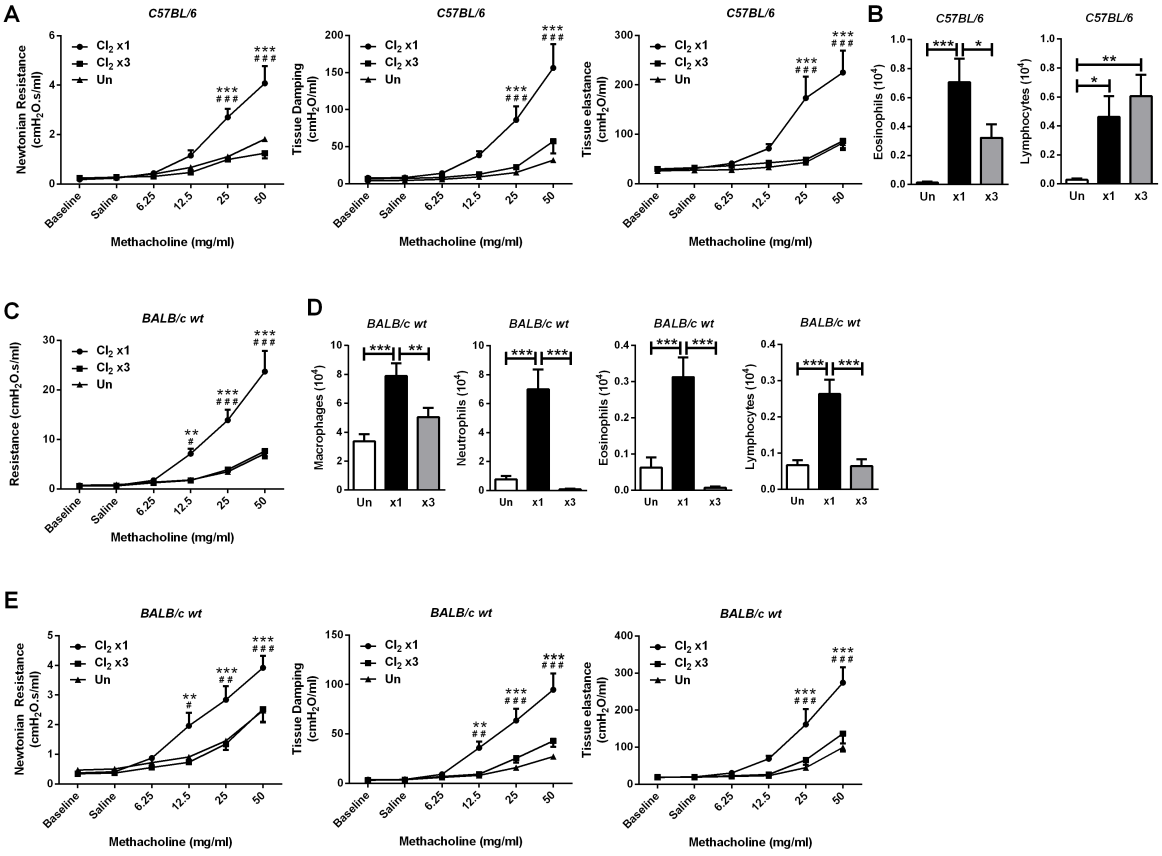
| Gene Symbol | Fold Change (linear) (Adapted vs. Naive) | ANOVA p-value (Adapted vs. Naive) | FDR p-value (Adapted vs. Naive) | Description |
|---|---|---|---|---|
| Thbs1 | 13,23 | 0,000079 | 0,05 | thrombospondin 1 |
| Itgam | 9,38 | 0,000080 | 0,05 | integrin alpha M |
| Mmp12 | 8,05 | 0,000088 | 0,05 | matrix metallopeptidase 12 |
| Adam8 | 7,07 | 0,000009 | 0,04 | a disintegrin and metallopeptidase domain 8 |
| AA467197; Mir147 | 6,20 | 0,000043 | 0,05 | expressed sequence AA467197; microRNA 147 |
| Msr1 | 4,79 | 0,000075 | 0,05 | macrophage scavenger receptor 1 |
| Ms4a4a | 4,67 | 0,000015 | 0,04 | membrane-spanning 4-domains, subfamily A, member 4A |
| Pla2g7 | 4,23 | 0,000024 | 0,04 | phospholipase A2, group VII |
| Slc6a8 | 3,68 | 0,000068 | 0,05 | solute carrier family 6, member 8 |
| Cxcl16 | 3,02 | 0,000002 | 0,02 | chemokine (C-X-C motif) ligand 16 |
| Cd63; Cd63-ps | 2,98 | 0,000006 | 0,03 | CD63 antigen; CD63 antigen, pseudogene |
| Pdpn | 2,76 | 0,000067 | 0,05 | podoplanin |
| Ptgs1 | 2,74 | 0,000001 | 0,02 | prostaglandin-endoperoxide synthase 1 |
| Fads1 | 2,48 | 0,000057 | 0,05 | fatty acid desaturase 1 |
| Apoe | 2,40 | 0,000060 | 0,05 | apolipoprotein E |
| Xdh | 2,11 | 0,000085 | 0,05 | xanthine dehydrogenase |
| AB124611 | 2,09 | 0,000054 | 0,05 | cDNA sequence AB124611 |
| Hmgcs1 | 2,08 | 0,000050 | 0,05 | 3-hydroxy-3-methylglutaryl-Coenzyme A synthase 1 |
| Rasa3 | 2,03 | 0,000082 | 0,05 | RAS p21 protein activator 3 |
| Ifitm2 | 2,02 | 0,000031 | 0,05 | interferon induced transmembrane protein 2 |
| | | | | |
| Rasgef1b | -2,11 | 0,000032 | 0,05 | RasGEF domain family, member 1B |
| Parp16 | -2,13 | 0,000057 | 0,05 | poly (ADP-ribose) polymerase family, member 16 |
| unknown | -2,33 | 0,000021 | 0,04 | |
| Treml4 | -2,7 | 0,000002 | 0,02 | triggering receptor expressed on myeloid cells-like 4 |
| Tnfsf13b | -3,47 | 0,000033 | 0,05 | tumor necrosis factor (ligand) superfamily, member 13b |
| Fabp1 | -3,85 | 0,000043 | 0,05 | fatty acid binding protein 1, liver |
| D630039A03Rik | -5,39 | 0,000004 | 0,03 | RIKEN cDNA D630039A03 gene |

ACCEPTED MANUSCRIPT

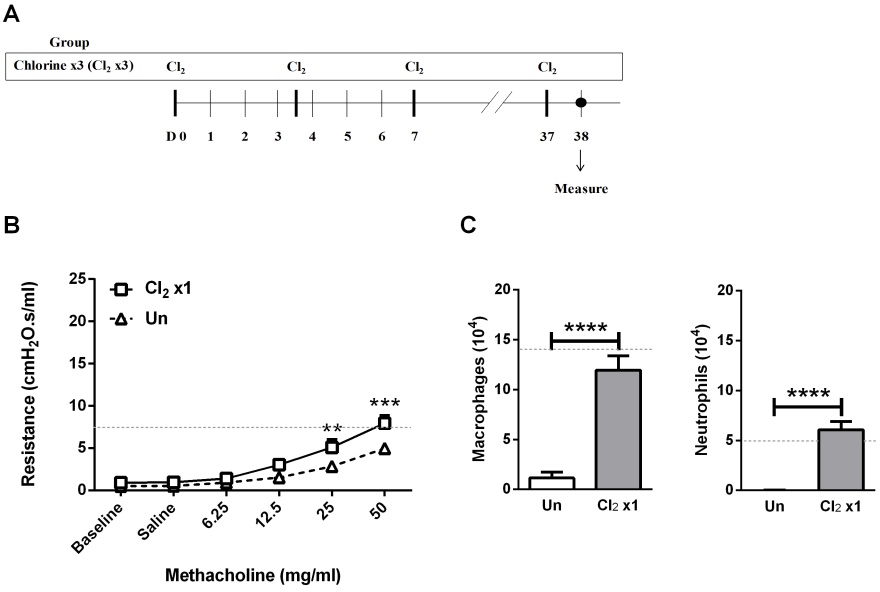
ACCEPTED MANUSCRIPT

| Gene Symbol | Role in resolution of inflammation, phagocytosis/efferocytosis or repair | FC | FDR | PMID |
|---|---|---|---|---|
| *Thbs1* | Thrombospondin is a multifaceted protein which may modulate the inflammatory process and impact its resolution, is involved in efferocytosis by facilitating the recognition and uptake of apoptotic cells, is a major activator of TGF-β1 and can promote resolution of experimental lung injury. | 13,2 | 0,05 | 21765615<br>21757719<br>9657149<br>24045574<br>1383273 |
| *Itgam* | Integrin alpha M (CD11b) might be expressed by alveolar macrophages following efferocytosis. | 9,4 | 0,05 | 21268007 |
| *Mmp12* | Matrix metalloproteinase-12 dampens inflammation and neutrophil influx in arthritis. | 8,1 | 0,05 | 25310974 |
| *Adam8* | Despite the risk of remodeling, a disintegrin and metallopeptidase domain 8 is involved in initiation of repair events in the airways. | 7,1 | 0,04 | 19255780<br>25480335 |
| *Mir147* | miR-147 prevents excessive inflammatory responses. | 6,2 | 0,05 | 19721002 |
| *Msr1* | Macrophage scavenger receptor 1 (Msr1, CD204) is involved in efferocytosis and is critical for the resolution of inflammation. | 4,8 | 0,05 | 18511575<br>15849212 |
| *Ms4a4a* | Ms4a4a is a novel marker of M2 pacrophages. | 4,7 | 0,04 | 22954708 |
| *Pla2g7* | Pla2g7 is coding for the lipoprotein-associated phospholipase A2 (Lp-PLA2) also known as platelet-activating factor acetylhydrolase (PAF-AH) described to reduce the lung inflammation. | 4,2 | 0,05 | 1997289<br>9230731<br>17629689 |
| *Slc6a8* | *Slc6a8* is coding for sodium and chloride-dependent creatine transporter 1. Creatine may have anti-inflammatory properties on endothelial cells, but his role on macrophages is unknown. | 3,7 | 0,05 | 12812994 |
| *Cxcl16* | Cxcl16 is mainly produced by alveolar macrophages in the airways. This chemokine is a mediator of angiogenesis, a first step through tissue repair, and may change the macrophage phenotype into M2 macrophages. | 3,0 | 0,02 | 16393323<br>26559672 |
| *Cd63* | CD63 is a member of the transmembrane 4 superfamily, also known as the tetraspanin family, often used as activation marker or marker of exosomes. | 3,0 | 0,03 | 26109643 |
| *Pdpn* | Podoplanin is involved in phagocytosis. | 2,8 | 0,05 | 20682314 |
| *Ptgs1* | Ptgs1 (or COX1 for cyclooxygenase-1) is the central enzyme in the biosynthetic pathway to prostaglandins from arachidonic acid. Macrophages that have ingested apoptotic cells inhibit proinflammatory cytokine production through autocrine/paracrine mechanisms involving prostaglandin E2. Prostaglandin may polarize macrophages and inhibit the inflammation. Recently, Yoon et al. demonstrated that macrophages programmed by apoptotic cells inhibit epithelial-mesenchymal transition in lung alveolar epithelial cells via prostaglandin. | 2,7 | 0,02 | 9466984<br>26931576<br>26875548 |
| *Fads1* | The protein encoded by the gene Fads1 is a member of the fatty acid desaturase (FADS) gene family which produce PGE2 and unsaturated fatty acids. Such unsaturated fatty acids are precursors to specialized pro-resolving mediators. For instance, Resolvins attenuate inflammation and promote resolution in cigarette smoke-exposed human macrophages. | 2,5 | 0,05 | 25857211<br>26301452 |
| *Apoe* | Apolipoprotein E (Apo E) is an immunomodulatory agent that polarizes macrophages in a M2 anti-inflammatory phenotype and suppresses the type I inflammatory response *in vivo*. Treatment by this apolipoprotein enhances phagocytosis by mononuclear phagocytes *in vitro*, and restores phagocytic activity and muscle regeneration in *Ccl2*$^{-/-}$ mice. | 2,4 | 0,05 | 21350196<br>26632270<br>11136731<br>16179587<br>15528376 |

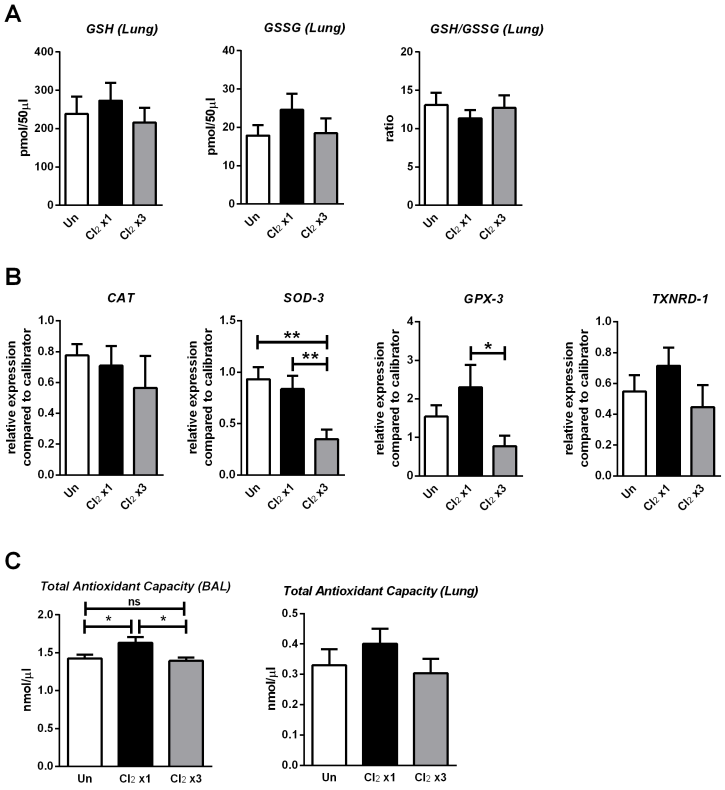
ACCEPTED MANUSCRIPT




ACCEPTED



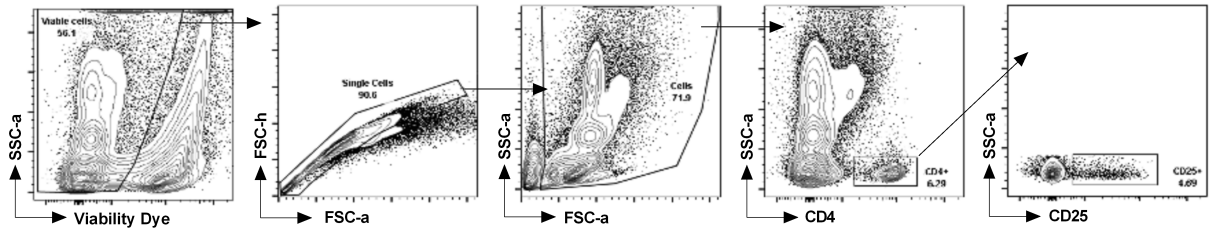

ACCEPTED MANUSCRIPT



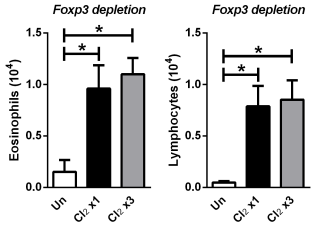

ACCEPTED MANUSCRIPT

ACCEPTED MANUSCRIPT

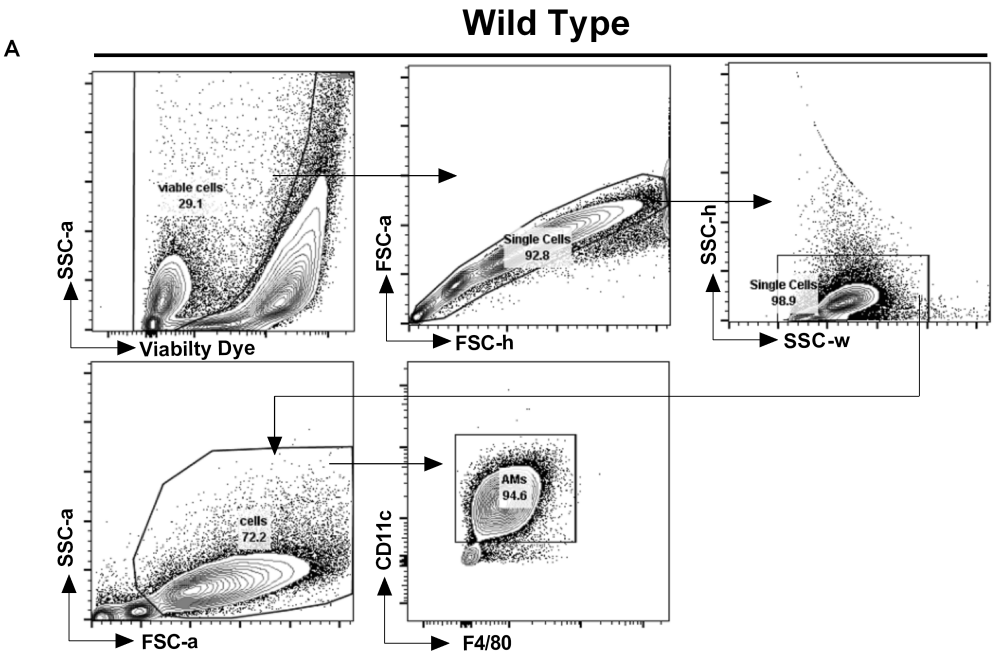
A

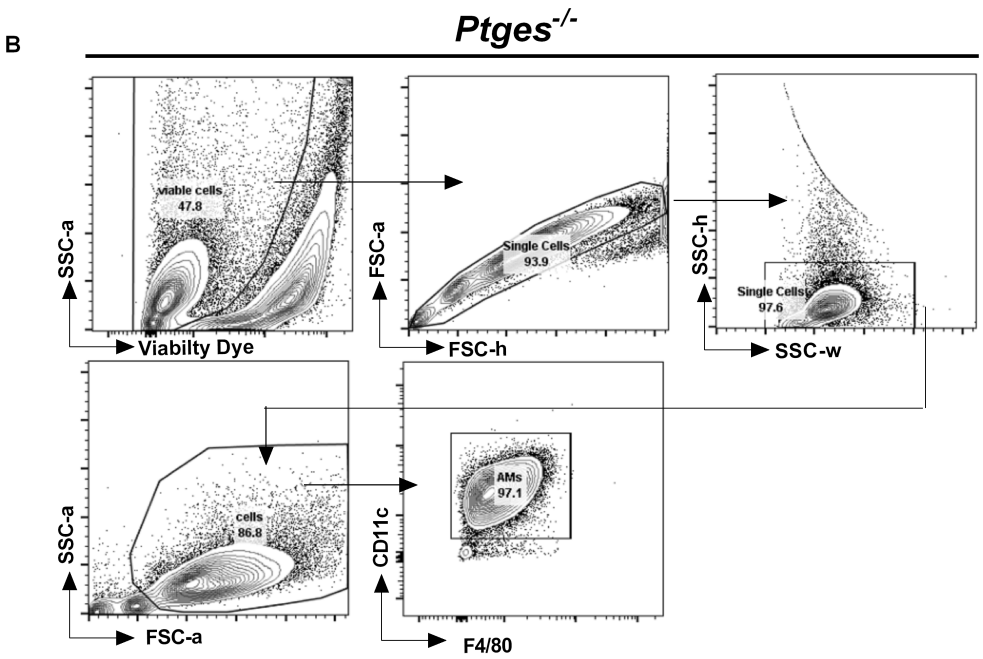


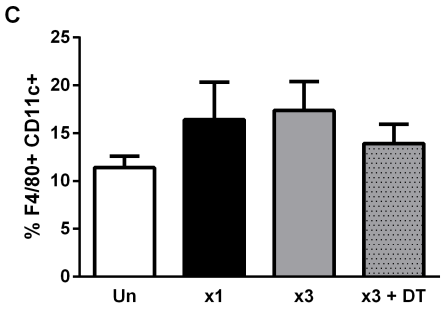

B

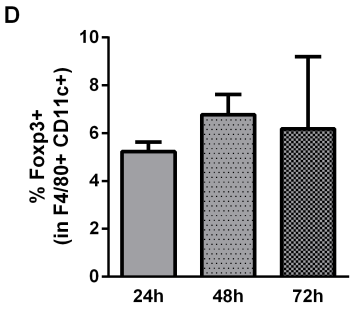


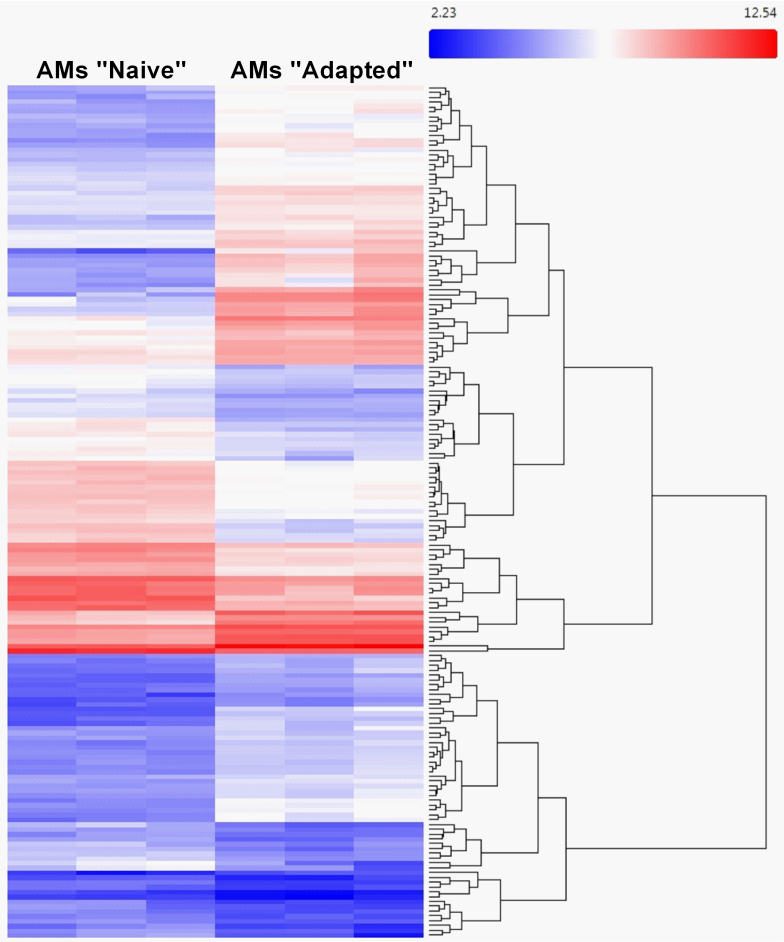

ACCEPTED MANUSCRIPT


A
Wild Type
viable cells
29.1
SSC-a
Viabilty Dye
Single Cells
92.8
FSC-a
FSC-h
Single Cells
98.9
SSC-h
SSC-w
cells
72.2
SSC-a
FSC-a
AMs
94.6
CD11c
F4/80

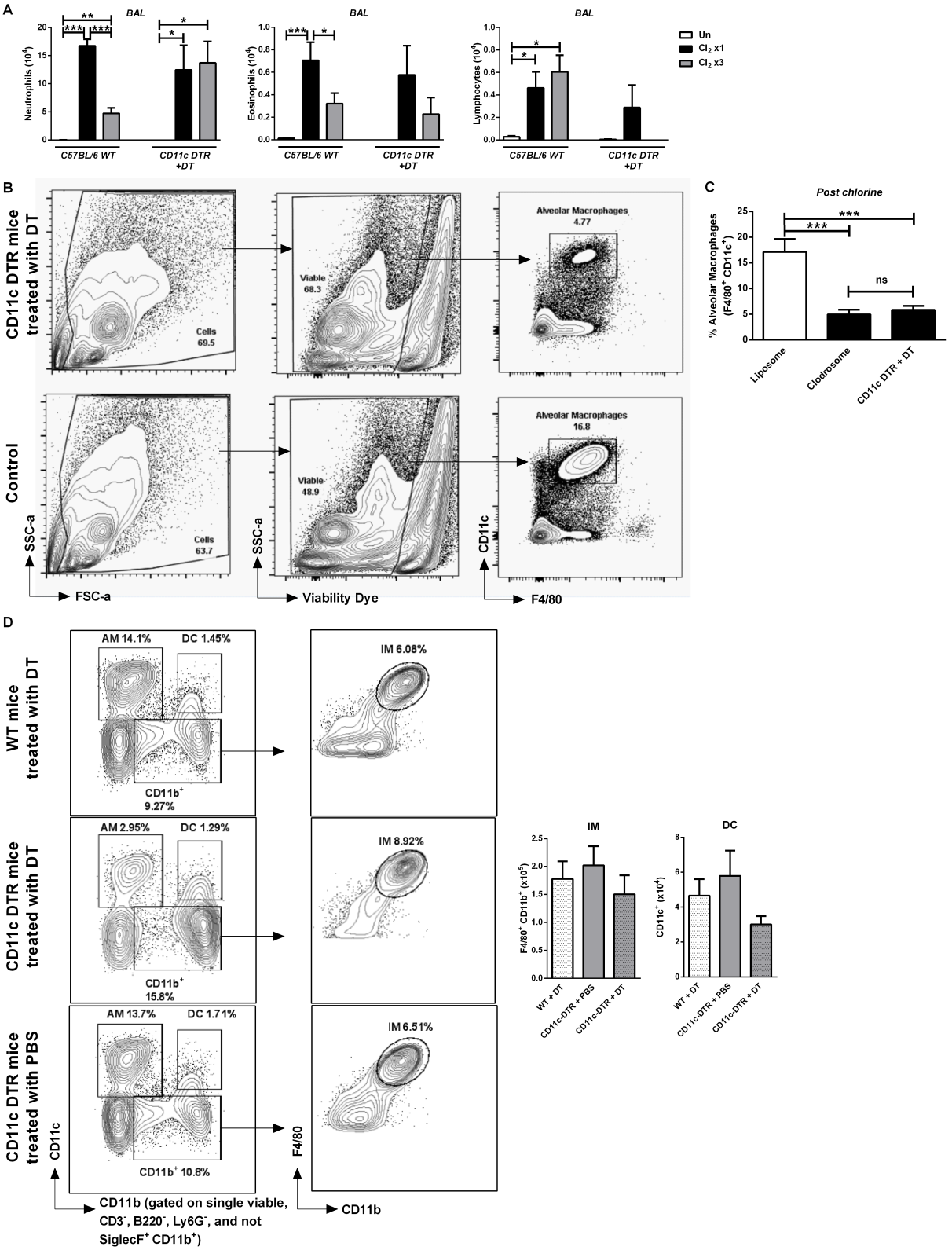

B
Ptges-/-
viable cells
47.8
SSC-a
Viabilty Dye
Single Cells
93.9
FSC-a
FSC-h
Single Cells
97.6
SSC-h
SSC-w
cells
86.8
SSC-a
FSC-a
AMs
97.1
CD11c
F4/80


C
% F4/80+ CD11c+
25
20
15
10
5
0
Un
x1
x3
x3 + DT


D
% Foxp3+
(in F4/80+ CD11c+)
10
8
6
4
2
0
24h
48h
72h




ACCEPTED MANUSCRIPT


A
BAL
Neutrophils (10⁴)
Eosinophils (10⁴)
Lymphocytes (10⁴)
Un
Cl2 x1
Cl2 x3
C57BL/6 WT
CD11c DTR +DT
B
CD11c DTR mice treated with DT
Control
Cells 69.5
Viable 68.3
Alveolar Macrophages 4.77
Cells 63.7
Viable 48.9
Alveolar Macrophages 16.8
SSC-a
FSC-a
Viability Dye
CD11c
F4/80
C
Post chlorine
% Alveolar Macrophages (F4/80⁺ CD11c⁺)
ns
Liposome
Clodrosome
CD11c DTR + DT
D
WT mice treated with DT
CD11c DTR mice treated with DT
CD11c DTR mice treated with PBS
AM 14.1%
DC 1.45%
CD11b⁺ 9.27%
IM 6.08%
AM 2.95%
DC 1.29%
CD11b⁺ 15.8%
IM 8.92%
AM 13.7%
DC 1.71%
CD11b⁺ 10.8%
IM 6.51%
CD11b (gated on single viable, CD3⁻, B220⁻, Ly6G⁻, and not SiglecF⁺ CD11b⁺)
IM
DC
F4/80⁺ CD11b⁺ (x10⁵)
CD11c⁺ (x10⁴)
WT + DT
CD11c-DTR + PBS
CD11c-DTR + DT

ACCEPTED MANUSCRIPT

**SUPPLEMENTAL MATERIALS**

**FIG E1. Lung function adaptation to oxidative injury in the different lung compartments and differential cell count**. (**A**) Resistance of central airways (Newtonian resistance, left panel) and peripheral airway (tissue damping, middle panel), and stiffness of the lung (tissue elastance, right panel) from C57BL/6 wild type mice (n=8/group pooled from 3 independent experiments). ***P<0.001 for $Cl_2$ x1 versus $Cl_2$ x3 and $^{###}$P< 0.001 for $Cl_2$ x1 versus Un (two-way ANOVA). (**B**) Absolute number of eosinophils and lymphocytes from bronchoalveolar lavage of C57BL/6 wild type mice (n=8/group pooled from 3 independent experiments). *P<0.05, **P<0.01, ***P<0.001 (one-way ANOVA). (**C**) Airway responsiveness to inhaled methacholine (Resistance) as measured in BALB/c wild type mice (n=7-9/group pooled from 4 independent experiments). **P<0.01, ***P<0.001 for $Cl_2$ x1 versus $Cl_2$ x3 and $^{#}$P<0.05, $^{###}$P< 0.001 for $Cl_2$ x1 versus Un (two-way ANOVA). (**D**) Absolute number of macrophages, neutrophils, eosinophils and lymphocytes (from left to right) from bronchoalveolar lavage of BALB/c wild type mice (n=7-9/group pooled from 4 independent experiments). **P<0.01, ***P<0.001 (one-way ANOVA). (**E**) Resistance of central airways (Newtonian resistance, left panel) and peripheral airway (tissue damping, middle panel), and stiffness of the lung (tissue elastance, right panel) in BALB/c wild type mice (n=6-9/group pooled from 4 independent experiments). **P<0.01, ***P<0.001 for $Cl_2$ x1 versus $Cl_2$ x3 and $^{#}$P<0.05, $^{##}$P<0.01, $^{###}$P< 0.001 for $Cl_2$ x1 versus Un (two-way ANOVA). Data are mean ± 1SEM.

**FIG E2. Adaptation to oxidative injury is persistent**. (**A**) One month after adaptation, adapted mice are subjected a new chlorine exposure or are unexposed. (**B**) Methacholine responsiveness (Resistance) and (**C**) cell count from bronchoalveolar lavage (macrophages and neutrophils) of adapted mice at 1 month. The dotted lines represent the level of response of mice after 3 chlorine exposures observed in figure 1. (n=8-9/group pooled from 3 independent experiments).

**FIG E3. Airway adaptation is independent of anti-oxidant response**. (**A**) Reduced glutathione (GSH, left panel), oxidized glutathione (GSSG, middle panel) and glutathione ratio (GSH/GSSG, right panel) in the lung. (**B**) Detoxifying enzymes mRNA (catalase, superoxide dismutase-3, glutathione peroxidase3, thioredoxin reductase-1; order from left to right) from lung tissue. (**C**) Total anti-oxidant capacity in the BAL (left panel) and lung (right panel). (n=5-6 BALB/c WT/group). *P<0.05, **P<0.01 (one-way ANOVA). Data are mean ± 1SEM.

**FIG E4. Gating strategy for regulatory T cells in DEREG mice and differential cell count.** (**A**) Gating strategy to obtain Tregs was as followed: viable cells (efluor780$^{-}$); single cells (FSC-A x FSC-H); all cells minus debris (FSC-A x SSC-A); CD4$^{+}$ cells (PerCP$^{+}$); CD25$^{+}$ cells (PE$^{+}$). See figure 4A for final step quantifying the level of Foxp3 expression. (**B**) Absolute number of eosinophils and lymphocytes from bronchoalveolar lavage of DEREG mice treated with diphtheria toxin (n=4-5/group pooled from 2 independent experiments). *P<0.05 (one-way ANOVA). Data are mean ± 1SEM.

**FIG E5. Gating strategy for monocytes/macrophages/dendritic cells and efficacy of depletion.** (**A**) Comparison of bronchoalveolar lavage inflammation between C57BL/6 wild type mice and CD11c DTR mice treated with diphtheria toxin. From left to right: neutrophils, eosinophils and lymphocytes (n=8/group pooled from 3 independent experiments for C57BL/6 wild type mice and n=4-6/group pooled from 3 independent experiments for CD11c DTR mice treated with diphtheria toxin). *P<0.05, **P<0.01, ***P<0.001 (one-way ANOVA). (**B**) Gating strategy to measure the efficacy of alveolar macrophage depletion in the airways of diphtheria toxin-treated CD11c DTR mice was as follows: cells minus debris (FSC-A x SSC-A), viable cells (efluor780$^{-}$); alveolar macrophages (F4/80-PECya7$^{+}$; CD11c-PerCP$^{+}$). (**C**) Quantification of alveolar macrophage depletion in clodronate-treated mice versus control liposome-treated mice and diphtheria-treated CD11c DTR-treated mice (n=7-10/group). ***P<0.001 (one-way ANOVA). (**D**) Gating strategy to evaluate the depletion of both dendritic cells (DC) and interstitial macrophages (IM) in air-exposed wild type mice treated with diphtheria toxin (40ng/g) and CD11c DTR mice treated with diphtheria toxin or PBS at 24h. (n=7-8/group pooled from 2 independent experiments). (one-way ANOVA). Data are mean ± 1SEM.

**FIG E6. FMO and gating strategy for alveolar macrophages from wild type and *Ptges*$^{-/-}$ mice.** The gating strategy in wild type (**A**) and Ptges$^{-/-}$ (**B**) mice was as followed: viable cells (efluor780); single cells (FSC-a x FSC-h); single cells (SSC-h x SSC-w); all cells less debris (FSC-a x SSC-a); alveolar macrophages (F4/80-PECya7$^{+}$; CD11c-PerCP$^{+}$). See figure 8B for the final step

quantifying Foxp3 expression in these cells. (**C**) Flow cytometry evaluation of the alveolar macrophage population in DEREG mice untreated or treated with diphtheria toxin (right side) (n=3-5 DEREG/group). (**D**) Foxp3 expression was measured by flow cytometry in the BAL of adapted mice at 24, 48 and 72 hours (n=3-5mice/group). Data are mean ± 1SEM.

**FIG E7. Gene expression from sorted alveolar macrophages from adapted mice.** Heat map of 34472 genes comparing alveolar macrophages from adapted and naïve mice (n=3/group, each n is a pool of 5-10 mice).

**Table E1. List of the 20 genes up-regulated and the 7 genes down-regulated in adapted alveolar macrophages.**

**Table E2. Immunosuppressive functions of the 15 genes up-regulated in adapted alveolar macrophages.** (FC: linear fold change, adapted vs naïve; FDR: false discovery rate, p-value, adapted vs. naïve; PMID: PubMed identifier).

ACCEPTED MANUSCRIPT